UNIVERSITAS INDONESIA

ANISOTROPIC PRESTACK DEPTH MIGRATION: A CASE STUDY IN VERTICAL TRANSVERSELY ISOTROPIC (VTI) MEDIA

BACHELOR THESIS

RINO ISMA ADITYA SAPUTRA
0706262716

FACULTY OF MATHEMATICS AND NATURAL SCIENCES
DEPARTMENT OF PHYSICS
DEPOK

MAY 2012

UNIVERSITAS INDONESIA

ANISOTROPIC PRESTACK DEPTH MIGRATION: A CASE STUDY IN VERTICAL TRANSVERSELY ISOTROPIC (VTI) MEDIA

BACHELOR THESIS

Submitted as partial fulfillment of the requirements for the degree of Bachelor of Science

RINO ISMA ADITYA SAPUTRA
0706262716

FACULTY OF MATHEMATICS AND NATURAL SCIENCES
DEPARTMENT OF PHYSICS
DEPOK
MAY 2012

HALAMAN PERNYATAAN ORISINALITAS

Skripsi ini adalah hasil karya sendiri,

dan semua sumber baik yang dikutip maupun dirujuk

telah saya nyatakan dengan benar.

Nama	: Rino Isma Aditya Saputra
NPM	: 0706262716
Tanda Tangan	: 
Tanggal	: 7 Mei 2012

SHEET OF APPROVAL

This bachelor thesis submitted by

Name	:	Rino Isma Aditya Saputra
Student number	:	0706262716
Study program	:	Physics
Title	:	Anisotropic Prestack Depth Migration: A Case Study in Vertical Transversely Isotropic (VTI) Media

Has been successfully defended before the Board of Examiners and declared acceptable as a partial fulfillment of the requirements for the Degree of Bachelor of Science in Physics at Department of Physics, Faculty of Mathematics and Natural Sciences, University of Indonesia.

BOARD OF EXAMINERS

Supervisor I : Dr. Eng. Supriyanto, M.Sc (.....)

Supervisor II : Ir. Hasan Nurudin, MT (.....)

Examiner I : Dr. Dede Djuhana, M.Si (.....)

Examiner II : Dr. Waluyo (.....)

Defense in : Depok
Date : May 7th, 2012

ACKNOWLEDGEMENT

First and foremost, I thank to Allah SWT the Almighty who has given me the ability to complete my bachelor thesis entitled "Anisotropic Prestack Depth Migration: A Case Study in Vertical Transversely Isotropic (VTI) Media".

This bachelor thesis has been written in partial fulfillment for the degree of Bachelor of Science in major subject Geophysics, Department of Physics, Faculty of Mathematics and Natural Sciences, University of Indonesia.

By this moment, let me address my special gratitudes to:

1. Dr. Eng. Supriyanto, M.Sc and Ir. Hasan Nurudin, MT as my supervisors, for their endless teachings, feedbacks and encouragements. Their willingness of providing time to give suggestions and review this work despite their workload enriched this thesis and will always be appreciated.
2. Dr. Dede Djuhana, M.Si and Dr. Waluyo as the examiners, for their constructive comments and excellent suggestions. Their review for this work had contributed the improvement to this bachelor thesis.
3. My beloved parents and my brothers, Rico and Reza, as well as my sister, Dahlia. I would probably not be writing this if it were not for the endless prayers and supports of them.
4. All geophysicists in PT. Elnusa Tbk who make pleasant condition for me as long as I work on my bachelor thesis there.
5. Bastian, Slamet, Inggrid, and Krisna Andita for their encouragement, scientific discussion and advices on many of the technical details. This bachelor thesis wouldn't be possible without you all.
6. All lecturers in University of Indonesia who open my eyes to look the beauty of sciences, particularly to Dr. rer. Nat. Abdul Haris who really support me to have priceless experiences.
7. Administration staffs of Department of Physics FMIPA UI, special thanks to Mbak Ratna for taking care of administrative necessities.

8. Liska, Togi, Andi, Yogi, Gamal, Alhada, Rezkia (Kiki), Yazid, Cumin, Fikar and Dian who accompany me as intern student in Elnusa, what a great moment there with you guys.
9. The five troops (Laskar 5), with whom I got this research finished together: Aji, Bahadur, Byan, Bundi, Edo, Gangga, Ichwan, Ferdy, Muladi, Rado, Rangga, Rismauly, Semok, Septian, Syahril, Torkis, Vaniardi, Wahid and Willem.
10. The big family of Geophysics and Physics grade 2007, really comfort to have friends like you with your genius jokes.
11. All UI students, particularly in Physics department, last five years at UI is one of the most important, exciting and enjoyable phase in my life. Jayalah selalu jaya!
12. Siska Afrianita, words would not be enough to express my gratitude to you.

I have received support, encouragement, and help from many people that I have not mentioned yet. But there are still some mistakes and imperfect work of me, in such way that all I need is many corrections and suggestions for the better work in the future.

Depok, May 2012

The Author

HALAMAN PERNYATAAN PERSETUJUAN PUBLIKASI TUGAS AKHIR UNTUK KEPENTINGAN AKADEMIS

Sebagai sivitas akademik Universitas Indonesia, saya yang bertanda tangan di bawah ini:

Nama	: Rino Isma Aditya Saputra
NPM	: 0706262716
Program Studi	: Geofisika
Departemen	: Fisika
Fakultas	: Matematika dan Ilmu Pengetahuan Alam
Jenis karya	: Skripsi

demi pengembangan ilmu pengetahuan, menyetujui untuk memberikan kepada Universitas Indonesia **Hak Bebas Royalti Noneksklusif (*Non-exclusive Royalty Free Right*)** atas karya ilmiah saya yang berjudul :

Anisotropic Prestack Depth Migration: A Case Study in Vertical Transversely Isotropic (VTI) Media

beserta perangkat yang ada (jika diperlukan). Dengan Hak Bebas Royalti Noneksklusif ini Universitas Indonesia berhak menyimpan, mengalihmedia/ format-kan, mengelola dalam bentuk pangkalan data (database), merawat, dan memublikasikan tugas akhir saya selama tetap mencantumkan nama saya sebagai penulis/pencipta dan sebagai pemilik Hak Cipta.

Demikian pernyataan ini saya buat dengan sebenarnya.

Dibuat di : Depok
Pada tanggal : 7 Mei 2012
Yang menyatakan

(Rino Isma Aditya Saputra)

ABSTRACT

Name : Rino Isma Aditya Saputra
Major : Physics
Title : Anisotropic Prestack Depth Migration: A Case Study In Vertical Transversely Isotropic (VTI) Media

The complex geological condition could be due to the structure-dependent such as diapiric structure or structure-independent such as facies changes. In that condition, the velocity of seismic wave has strong lateral velocity variation. In order to image that condition properly, depth migration is the appropriate way to be performed. Unfortunately, the use of conventional PSDM generally takes the isotropy assumption, not anisotropy like the real subsurface condition. As the result, the isotropy assumption yields inaccurate interval velocity in model building stage. If the interval velocity is inaccurate, the PSDM yields hockey stick effect in the depth gather as well as miss-tie between seismic horizons against well markers. In respect to those issues, anisotropic assumption should be considered by inserting Thomsen's parameters in PSDM process.

This study shows how Thomsen's parameters, δ and ε, play the role in vertical transverse isotropy (VTI) media. The δ parameter is the degree of anisotropy of P-wave in near-vertical direction while ε is the degree of anisotropy of P-wave in near-horizontal direction. The Thomsen's parameter is obtained by calculation of the relationship between well-markers and seismic horizons. Both Thomsen's parameters are aims to correct the depth level and flatness of the depth gather. The δ parameter is also used into anisotropic velocity transformation. The Anisotropic PSDM is performed iteratively by refining the anisotropic interval velocity, δ and ε until the flat reflection event at the depth gather, even at the far-offset, acquired.

By involving the Thomsen's parameters in PSDM process, it corrects the hockey stick effect and yields proper image rather than isotropic PSDM. The result of anisotropic PSDM is reflected by removing miss-tie between well-markers against seismic horizons, shows the clear fault pattern as well as the strong and continuous reflector event in stack section.

Keywords : Anisotropy, Thomsen's Parameter, VTI, prestack depth migration, interval velocity model.
xiii + 68 pages : 44 pictures; 2 tables
Bibliography : 23 (1971-2010)

ABSTRAK

Nama : Rino Isma Aditya Saputra
Program Studi : Fisika
Judul : *Prestack Depth Migration* Anisotropi: Studi Kasus pada Media *Vertical Transversely Isotropic (VTI)*

Kondisi geologi bawah permukaan yang kompleks dapat dikarenakan oleh *structure-dependent* seperti struktur diapir ataupun *structure-independent* seperti perubahan *facies* suatu lapisan. Pada kondisi geologi yang seperti itu, kecepatan gelombang seismic akan mempunyai variasi kecepatan yang kuat. Untuk mencintrakan kondisi bawah permukaan seperti itu dengan baik, *depth migration* adalah cara yang tepat untuk dilakukan. Sayangnya, penggunaan PSDM konvensional umumnya masih menggunakan asumsi homogen isotropik, bukan anisotropik layaknya kondisi bawah permukaan yang sebenarnya. Asumsi tersebut yang membuat model kecepatan interval yang dihasilkan kurang tepat. Ketika model kecepatan interval kurang tepat, maka hasil *image* dari *isotropic* PSDM masih kurang optimum dan menyebabkan adanya efek *hockey stick* serta *miss-tie* antara horizon pada seismik dengan *marker* pada sumur sebagai referensi. Terkait dengan masalah tersebut, asumsi anisotropi dapat dilibatkan didalam proses PSDM dengan memasukan parameter Thomsen.

Pada tugas akhir ini akan ditunjukan bagaimana parameter Thomsen, yaitu δ dan ε, berperan pada kasus vertical transverse isotropy (VTI). Parameter delta, δ, merupakan derajat anisotropi gelombang P untuk arah *near-vertical* sedangkan epsilon, ε, merupakan derajat anisotropi gelompang P untuk arah *near-horizontal*. Parameter Thomsen didapat dari perhitungan hubungan antara seismik horizon dan *marker* pada sumur. Kedua parameter Thomsen bertujuan untuk mengkoreksi level kedalaman dan tingkat kelurusan reflektor pada *gather*. Parameter δ juga digunakan dalam proses transformasi kecepatan interval anisotropi. PSDM anisotropi sendiri dilakukan secara iteratif dengan memperbaiki model kecepatan anisotropi, δ dan ε hingga reflektor pada data gather sudah lurus hingga *far-offset.*

Dengan melibatkan parameter anisotropi ke dalam proses PSDM, akan mengkoreksi efek *hockey stick* serta hasil yang didapat lebih baik dibandingkan dengan *isotropic* PSDM. Hasil dari PSDM anisotropi ditunjukan dengan menghilangkan *miss-tie* antara *marker* pada sumur dan horizon pada seismic, menunjukan pola patahan yang jelas serta menghasilkan reflektor yang lebih jelas dan kontinu pada *stack section*.

Kata Kunci : Anisotropi, Parameter Thomsen, VTI, *prestack depth migration*, model kecepatan interval.
xiii + 68 halaman : 44 gambar ; 2 tabel
Daftar Pustaka : 23 (1971-2010)

TABLE OF CONTENTS

LIST OF FIGURES

LIST OF TABLES

CHAPTER 1
INTRODUCTION

1.1 Background

Seismic velocity varies laterally and/or horizontally if it deals with complex geological condition. Strong lateral velocity variation in complex geological condition is associated with structure-dependent (ex: diapiric structure) and structure-independent (ex: associated with facies changes). In order to image properly that condition, appropriate imaging strategies should be designed. The good quality of seismic section is as consequence of velocity used. As one of the imaging strategies, time migration is only adequate for imaging the target that has velocity variation mild to moderate. The velocity model used in time migration, RMS velocity, is not able to determine velocity complex geological condition. In the other side, depth imaging that using interval velocity can define the velocity of each layer properly. Due to the difference of velocity model used, depth migration, particularly prestack depth migration, has relatively superiority in imaging rather than time migration. Depth imaging greatly extends the ability to image geologic structure. It is these benefits, vertical positioning, lateral positioning, resolution and velocity estimation, which are responsible for the successes of depth imaging (Fagin, 2002).

The success of depth imaging is not perfectly obtained once one considers the isotropic media in the process of depth imaging. In most applications of elasticity theory to problems in term of petroleum geophysics, the elastic medium is assumed to be isotropic. In fact, most crustal rocks are found experimentally to be anisotropic. Further, it is known that if a layered sequence of different media (isotropic or not) is probed with an elastic wave of wave length much longer than the typical layer thickness (i.e., the normal seismic exploration context), the wave propagates as though it were in a homogeneous, but anisotropic, medium (Backus, 1962). Therefore, there is a fundamental inconsistency between practice on the one hand and reality on the other (Thomsen, 1986).

The isotropic assumption causes the presence of *hockey stick* effect which obviously seen at the far offset of seismic gather. As the consequence of hockey stick existence, the quality of seismic section while stacked not yields the optimum result. In addition, the velocity model that obtained by isotropy assumption is not the appropriate model and it affects the depth of reflector event, seismic horizon, in the seismic stack section unmatched to well-marker. Therefore, in the process of depth imaging, the reflector event in the gather is needed to be flattened by achieving the accurate interval velocity model. In that case, Thomsen's parameters is the solution in order to solve that problem.

This study conducts the involvement of Thomsen's parameters, δ and ε, into the PSDM process which implemented to vertical transversely isotropic (VTI) media. It has focus on matching the horizon seismic against well-marker as well as comparing between isotropy section and anisotropy section to look the improvement. That concerns is achieved by performing anisotropic prestack depth migration. It plays a crucial role in yielding seismic image which represent the true geological condition. However, the result of anisotropic PSDM helps to recognize the geological condition more detail and reliable as well as diminish the misplaced reflector in the stack section.

1.2 Objectives

This research has some objectives to reach to, those are:

1. Obtaining the geological subsurface model that represent true geological condition.
2. Involving anisotropy parameter to build the interval velocity model in order to tie the seismic data against well data.
3. Comparing the result of Isotropic PSDM to anisotropic PSDM in VTI media, which the differences of image quality and reflector position can be obviously seen.
4. In partially fulfillment of the requirements for the degree of Bachelor of Science, Department of Physics, Faculty of Mathematics & Natural Sciences, University of Indonesia.

1.3 Problem Limitation

This research focused on:

1. Data limited to 2-D seismic with 1 well.
2. Using PSTM section, RMS velocity section, and CMP gather as the input of isotropic PSDM then continued to anisotropic PSDM.
3. The analysis is focused on the result of isotropic PSDM and Anisotropic PSDM.
4. Processing the data using GeoDepth EPOS3TE software from Paradigm.

1.4 Research Methodology

In order to reach those objectives with fine-quality result as expected, this research will do the following steps:

1. Problem identification and determining research objectives.
2. Literature Review

   Comprise to reference books reading, related papers/publication, and software review which particularly related to PSDM and seismic anisotropy.
3. Data Preparation

   This is the basic 2D seismic data interpretation which is horizon picking. The data used as input are PSTM section, RMS velocity section, time gather, and well data.
4. Data Processing and Modeling

   It will be divided into 3 main steps, which are:
   - Create initial isotropy model with layer stripping method which building structure and velocity model. Velocity model is created using Dix conversion for the first layer and Coherency Inversion for the rest of the layers. After the initial model obtained, run isotropic PSDM using Kirchhoff (wave front) algorithm.

- Create refinement isotropy model to refine the initial model by picking residual move-out and using horizon-based tomography. After the refinement model obtained, run isotropic PSDM using Kirchhoff (wavefront) algorithm.
- Create anisotropy model by inserting anisotropy parameter where the anisotropy parameter is calculated based on seismic horizon and well-marker. After anisotropy model obtained, run isotropic PSDM using Kirchhoff (wave front) algorithm.

5. Comparing and Analyzing Result
   It compares the results of isotropic PSDM and anisotropic PSDM.

1.5 Bachelor Thesis Structures

Systematically, this bachelor thesis will be divided into 5 chapters, each of them comprise to several parts. Summary of those chapters would be like this below:

- Chapter 1 explains about background and the objectives of this research, scope of study, and the methodology that will be used.
- Chapter 2 explains basic theory that related to this research such as basic concept of seismic reflection, migration, prestack depth migration and seismic anisotropy.
- Chapter 3 explains the methodology which consists of initial velocity model building, isotropic PSDM, refinement velocity model using analysis residual-moveout as well as horizon-based tomography, and anisotropic PSDM.
- Chapter 4 explains the result and analysis of isotropic and anisotropic PSDM.
- Chapter 5 consists of conclusions and recommendations that will summarize this research and give some recommendations for the better future work.

CHAPTER 2
BASIC THEORY

This chapter explains the basic concept of seismic wave, migration, depth imaging and seismic anisotropy. The first part is basic concept of seismic wave, it consists of the rules of raypath, types of seismic waves, and the theory of elasticity. The second part is basic concept of migration which consists of migration strategies and Kirchhoff algorithm. The third part is depth imaging, it is divided into two stage which are initial model building and model refinement. The last part is seismic anisotropy, it consists of types of anisotropy and anisotropic velocity analysis.

2.1 Theory of Seismic Wave

2.1.1 The Rules of Ray Path

- **Fermat Principle**

Basically, the seismic wave propagating through a medium is according to Fermat principle. Fermat's principle explains that a wave will take that raypath for which the traveltime is stationary with respect to minor variations of the raypath, that is, for which the change in the traveltime for an incremental change in raypath is zero. For most situations the raypath involves the minimum traveltime, that is, travel over any neighboring path will take longer; hence Fermat's principle is often called the principle of least time or the brachistochrone principle. Snell's law, Huygens' Principle, and many other laws of geometrical optics can be derived from this principle (Sheriff, 1995). In formal statement, the traveltime along a raypath from one point to another has an extremum value which, for most physical problems, is a minimum (Officer, 1958). The raypath geometry depicted in figure 2.1.

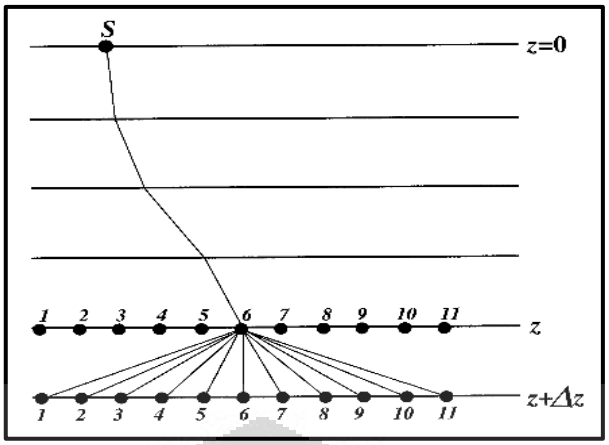

Figure 2.1 Sketch that illustrates the ray path (Yilmaz, 2001)

- **Huygens Principle**

Huygens principle is important in understanding wave travel and is often useful in drawing successive positions of wavefront. Huygens principle states that every point on a wavefront can be regarded as a new source of waves (Sheriff, 1995).

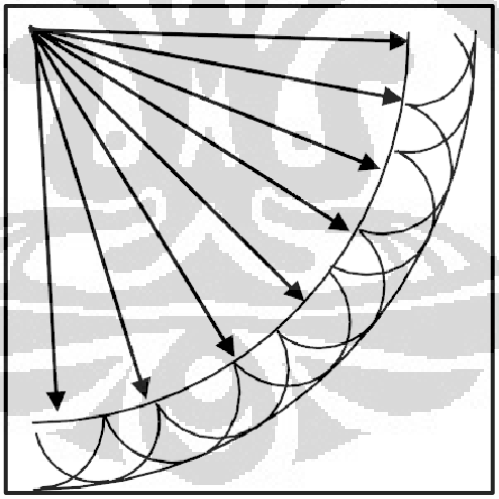

Figure 2.2 Huygens principle (Yilmaz, 2001)

As the wave propagates the seismic energy is distributed over an ever increasing spherical surface. The wavefront is circular while the velocity remains constant. In the case of constant velocity media, assuming the source is located on the top and we only consider the horizontal and downgoing directions, they are semicircles. In 3D point of view, it seems as hemispheres.

- **Snell's law**

Fermat principle is used as the basic concept of Snell's law. In isotropic medium whereas the velocity is constant, the raypath takes the straight path or shortest distance. Figure 2.3 portrays the wave propagates across 2 layers of different velocities. The raypath bend as they cross the velocity interfaces. Raypaths bend toward the interface normal as they enter low-velocity media and away from the normal as they enter high velocity material.

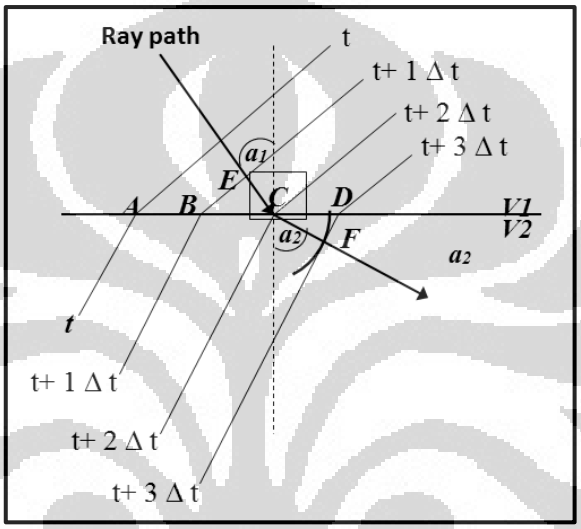

Figure 2.3 Ray path bend in accordance with Snell's law

By a sketch in Figure 2.3, it can be mathematically defined as:

$$Sin\,(a_1) = \frac{EC}{BC} \tag{2.1}$$

$$Sin\,(a_2) = \frac{CF}{CD} \tag{2.2}$$

$$CF = \Delta t\,.V2 \tag{2.3}$$

$$EC = \Delta t\,.V1 \tag{2.4}$$

As can be seen$BC = CD$, thus

$$\frac{Sin\,(a_1)}{\Delta t\,.V1} = \frac{Sin\,(a_2)}{\Delta t\,.V2} \tag{2.5}$$

It can be simplified that

$$\frac{Sin\,(a_1)}{V1} = \frac{Sin\,(a_2)}{V2} \tag{2.6}$$

Equation (2.6) is the law of reflection and law of refraction, also well known as Snell's law.

2.1.2 Types of Seismic Waves

In general form, wave equation can be written as:

$$\frac{1}{V^2}\frac{\partial^2\psi}{\partial t^2} = \nabla^2\psi \tag{2.7}$$

The quantity ψ has not been defined; we have merely inferred that it is some disturbance that is propagated from one point to another with speed *V*. However, in a homogeneous isotropic medium, we have two relations:

$$\frac{1}{\alpha^2}\frac{\partial^2\Delta}{\partial t^2} = \nabla^2\Delta, \tag{2.8}$$

Where

$$\alpha^2 = \frac{(\lambda + 2\mu)}{\rho}$$

And

$$\frac{1}{\beta^2}\frac{\partial^2\theta_x}{\partial t^2} = \nabla^2\theta_x, \tag{2.9}$$

Where

$$\beta^2 = {}^{\mu}/_{\rho}$$

Equation (2.8) and (2.9) must be satisfied. It can be identified the functions θ and Δ, with ψ and conclude that two types of waves can be propagated in a homogeneous isotropic medium, one corresponding to changes in the dilatation Δ and the other to one or more components of the rotation.

The first type is variously known as a *dilatational, longitudinal, rotational, compressional,* or P-*wave* the latter name being given because this type is usually the first (primary) event on an earthquake recording. The second type is referred to as the *shear, transverse, rotational,* or S-w*ave* (because it is usually the second major event observed on earthquake records). The P-wave has

the velocity α in equation (2.8) and the S-wave the velocity β in equation (2.9), that is,

$$\alpha = \left(\frac{\lambda+2\mu}{\rho}\right)^{1/2} = \left(\frac{M}{\rho}\right)^{1/2} \tag{2.10}$$

$$\beta = \left(\frac{\mu}{\rho}\right)^{1/2} \tag{2.11}$$

where M is the P-wave modulus. Because the elastic constants are always positive, α is always greater than β.

Both of P-wave and S-wave are classified as body wave. In the other side, there is surface wave once the wave propagating around surface. Surface wave itself is plane waves that traveling parallel to the x-axis with velocity V and amplitude decreasing exponentially with distance from the *xy*-plane. Such waves are called surface waves because they are "tied" to the surface and diminish as they get farther from the surface (Sheriff, 1995). Love wave, Rayleigh wave, Stoneley wave, and tube wave are classified as surface wave.

2.1.3 Theory of Elasticity

The wave propagation through earth depends upon the elasticity properties of rocks. The shape and size of a material, even a solid body such as rocks, can be changed by applying external force. When the external force is removed, there are materials that able to return to its original condition and materials that getting permanent deformation. The property of resisting changes in terms of size or shape and returning to the undeformed condition when the external forces are removed is called elasticity (Sheriff, 2001).

The relation between applied forces and the deformation are conveniently expressed in terms of the concepts stress and strain. Stress, force per unit area, is divided into normal stress and shear stress. Figure 2.4 portrays the stress and strain that perform on the square. Meanwhile, Strain is the deformation of a material due to stress. It can be also defined as the amount of deformation an object compared to its original size and shape. Strain is classified into three types which are linear strain, volume strain and shear strain.

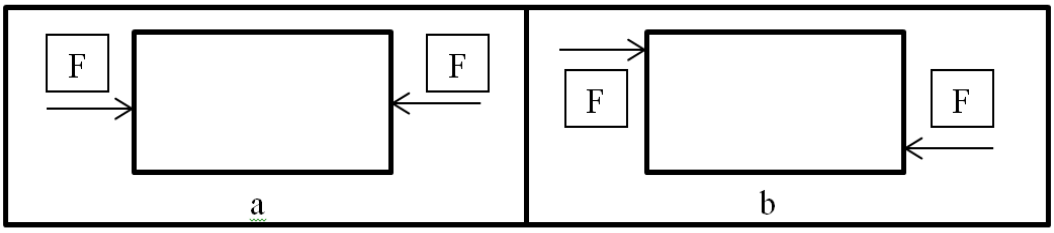

Figure 2. 4 a) normal stress b) shear stress

Hooke's law states the relation between stress-strain in elastic solid that the strain at any point is directly proportional to the stress applied at that point. Mathematically, Hooke's law can be expressed as $P = Ce$, where P = stress ; C=elastic constant ; and e = strain.

Elastic constant, or modulus, is a constant that describe the stress-strain relation. The elastic constant or modulus that represents a deformation of material is divided into:

a) Bulk modulus, B or 1/k, is the ratio of hydrostatic stress to volumetric strain; hence, it is a measure of incompressibility. Mathematically it can also be expressed as $B = \frac{-\Delta p}{\Delta V/V}$, where Δp is the pressure change, k is compressibility, ΔV is the volume change, and V is the initial volume.

b) Modulus of rigidity, M, is the ratio of shear stress to shear strain; hence, it is a measure of resistance to shear stress. Mathematically, it can be expressed as $M = \frac{shear\ stress}{shear\ strain}$.

c) Young's modulus, E, is the ratio of the longitudinal stress to the longitudinal strain associated with a cylindrical rod that is subjected to a longitudinal extension in the axial direction. Since strain is a dimensionless quantity, Young's modulus has the dimension of stress. In math form, $E = \frac{longitudinal\ stress}{longitudinal\ strain}$.

d) Poisson's ratio, σ, is the ratio of the lateral contraction to longitudinal extension associated with a cylindrical rod that is subjected to a longitudinal extension in the axial direction. Since

strain is a dimensionless quantity, Poisson's ratio is a pure number. In math form, $\sigma = \frac{stress\ transversal}{strain\ longitudinal}$.

2.2 Basic Concept of Migration

Migration moves dipping reflections to their true subsurface positions and collapses diffractions, thus increasing spatial resolution and yielding a seismic image of the subsurface (Yilmaz, 2001). In simple words, migration is aims to produce the stacked section appear similar to the geological condition.

The following observations can be made from the geometric description of migration (Yilmaz, 2001):

a) The dip angle of the reflector in the geologic section is greater than in the time section; thus, migration steepens reflectors.
b) The length of the reflector, as seen in the geologic section, is shorter than in the time section; thus, migration shortens reflectors.
c) Migration moves reflectors in the updip direction.

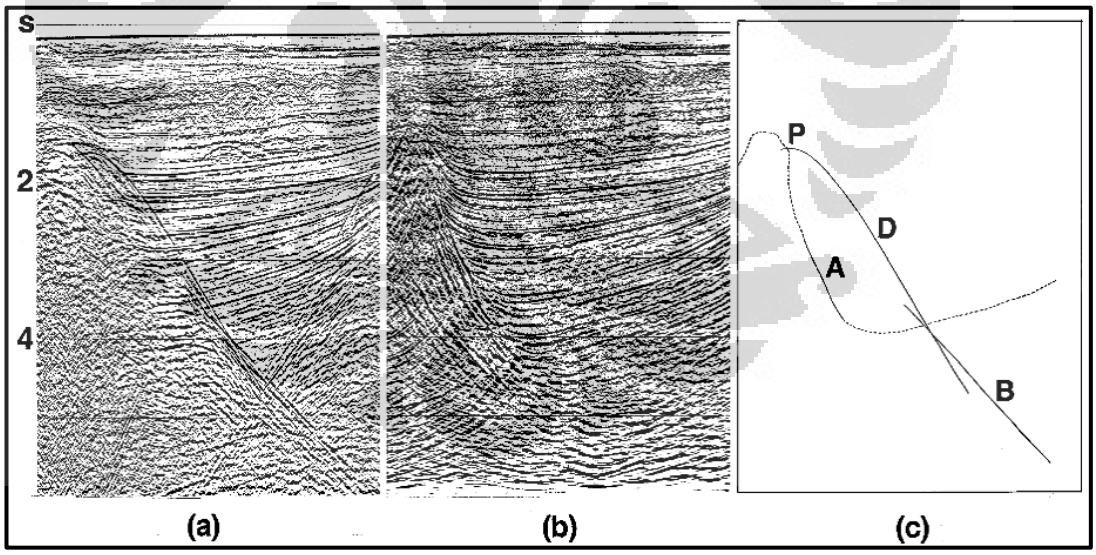

Figure 2.5 A CMP stack (a) before migration, (b) after migration, (c) sketch of a prominent diffraction D and a dipping event before and after migration.

Figure 2.5 portrays the example of seismic section before and after stack. Migration moves the dipping event B to its assumed true subsurface position A and collapses the diffraction D to its apex P.

When a stacked section is migrated, the migration theory applicable to data recorded with a coincident source and receiver (zero-offset). The recorded energy follows raypaths that are normal incidence to reflecting interfaces. Actually, this recording geometry obviously is not realizable in practice.

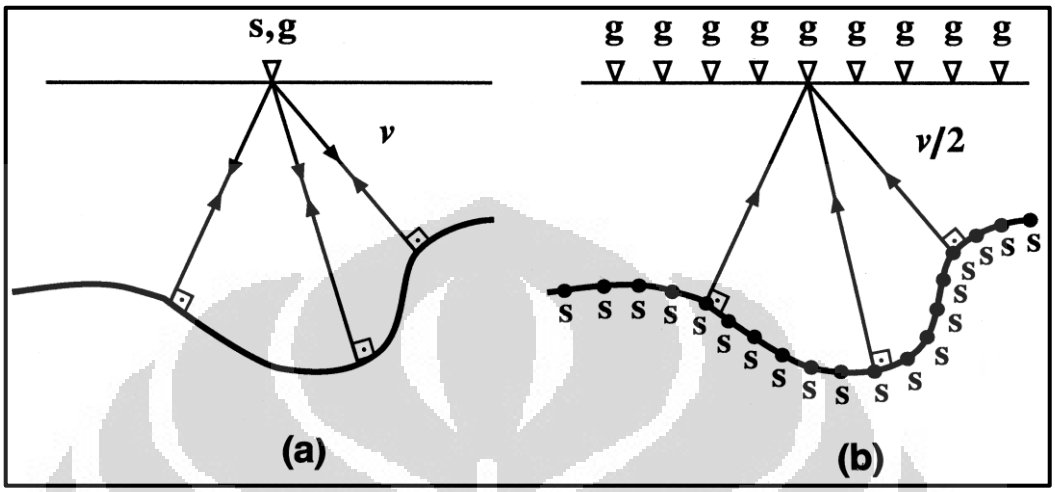

Figure 2.6 Geometry of zero-offset recording (a), and hypothetical simulation of the zero-offset experiment using exploding reflectors (b). (Claerbout, 1985).

Now consider the alternative geometry that can yield the same stacked section like zero-offset assumption. Imagine exploding sources that are located along the reflecting interfaces (Lowenthal et al., 1976). Also consider one receiver located on the surface at each CMP location along the line. The velocity of propagation is half of the true mdium velocity for the exploding reflectors model.That new model is referred as the *exploding reflector model*. The velocity of propagation is half of the true mdium velocity for the exploding reflectors model. Figure 2.6 shows the geometry of zero-offset recording (left) and exploding reflector model (right).

The equivalence between the zero-offset section and the exploding reflectors model is not quite exact, particularly in the presence of strong lateral velocity variations (Kjartansson and Rocca, 1976). These concepts now are applied to the velocity-depth model in Figure 2.7. It can be seen that there is bowtie effect on the right side of Figure 2.7.

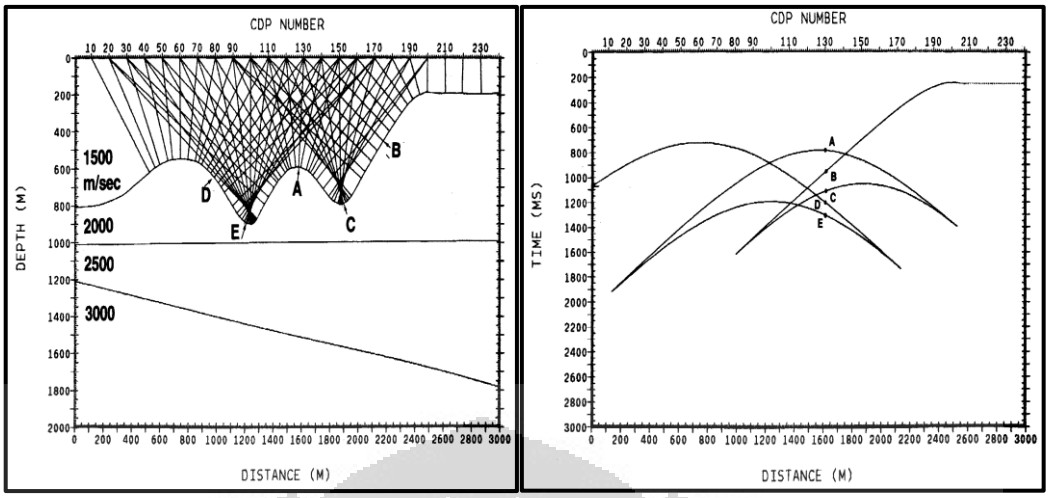

Figure 2.7 A velocity-depth model (left) and the zero-offset travel time response (right) of the weater-bottom reflector (Yilmaz,2001).

Figure above also shows the normal-incidence rays used to compute the zero-offset travel time trajectory. The question comes out regarding the validity assumtion that stacked section is equivalent to a zero-offset section. The conventional recording geometry provides the wavefields at nonzero offsets. During processing, the offset axis, by stacking the data onto the midpoint-time plane at zero offset is collapsed. For CMP stacking, hyperbolic moveout is normally assumed. It is no longer true for some reflections on some CMP gathers once the data present of the presence of strong lateral velocity variations. The assumption that conventional stacked section is equivalent to a zero-offset section also is violated to varying degrees in the presence of strong multiples and conflicting dips with different stacking velocities (Yilmaz, 2001).

2.2.1 Migration Strategies

The consideration of performing migration depends on (Yilmaz, 2001):

a) 2-D versus 3-D migration,
b) post- versus prestack migration, and
c) time versus depth migration

The spectrum of migration strategies extend from 2-D poststack time migration to 3-D prestack depth migration. An appropriate migration strategy depends on the nature of subsurface geology. Time migration is able to deal with lateral velocity variation from mild to moderate. In contrast, depth migration is able to deal with the velocity that extremely varies laterally and/or horizontally.

After the strategy of migration selected, some aspects should be considered in order to obtain the optimum result of migration such as Migration algorithms, parameter, aspect of input data, and migration velocities.

The migration algorithm is aims to handle steeps dip with sufficient accuracy as well as the lateral and vertical velocity variations. The basis of common migration algorithms is one-way-depth scalar wave equation, equation (2.7). These algorithms do not explicitly model multiple reflections, converted wave, surface wav, or noise. Migration algorithms can be classified under three main categories (Yilmaz, 2001):

a) the *integral solution* to the scalar wave equation (ex: Kirchhoff migration),
b) the *finite-difference* solutions (ex: wave equation migration),
c) the *frequency-wave number* implementations (ex: Stolt migration).

In addition, the each of migration algorithms has various parameters in the process of migration. This parameter also plays the role in yielding the quality of stacked section image. The following parameters are the critical parameter of migration algorithm (Yilmaz, 2001):

a) Kirchhoff migration has the critical parameter which is the aperture width. A small aperture causes removal of steep dips; it generates spurious horizontal events and organizes the random noise uncorrelated from trace to trace.
b) Depth step size in downward continuation is the critical parameter in finite-difference methods. An optimum depth step size is the largest depth step with the minimum tolerable phase errors. It depends on temporal and spatial samplings, dip, velocity, and frequency. It also depends on the type of differencing scheme used in the algorithm.

c) Stolt migration that utilize frequency-wavenumber implementation has the critical parameter which is stretch factor A constant-velocity medium implies a stretch factor of 1. In general, the larger the vertical velocity gradient, the smaller the stretch factor needs to be.

The various aspects of input data set needs to concern pertain to line length or areal extent, spatial aliasing, and signal-to-noise ratio.In complex geology, a short record profiles result a fatal error while the line length is not sufficient. The line length must be sufficient to allow a steeply dipping event to migrate to its true subsurface location. Not only line length that has obstacles once meet steep dips event or complex geology, trace spacing must be somewhat small in order to prevent spatial aliasing. The presence of noise must be pushed as minimum as possible, both linear and random. It can be hazardous in processing the data, particularly in estimating the velocity.

Velocity is the key factor of migration process. Accuracy in event positioning and the image quality of stacked section after performing migration depends on migration algorithm used and velocity errors. Based on equation 2.12, 2.13, and 2.14 (Chun and Jacewitz, 1981) where the velocity generally increases with depth, errors in migration are usually larger in deep events than shallow events. The equation is to examine the vertical and horizontal displacements in the migrated time domain.

$$d_x = \frac{v^2 t}{4}\frac{\Delta t}{\Delta x}, \tag{2.12}$$

$$d_t = t\left[1 - \sqrt{1 - \left(\frac{v\Delta t}{2\Delta x}\right)^2}\right] \tag{2.13}$$

$$\frac{\Delta \tau}{\Delta x} = \frac{\Delta t}{\Delta x}\frac{1}{\sqrt{1-\left(\frac{v\Delta t}{2\Delta x}\right)^2}} \tag{2.14}$$

The horizontal (offset) and vertical (time) displacements – d_x and d_t,and the dip $\frac{\Delta \tau}{\Delta x}$, all measured on the migrated time section, can be expressed in terms of medium velocity v, traveltime t, and apparent dip $\frac{\Delta t}{\Delta x}$ as measured on the unmigrated time section.

2.2.2 Kirchhoff Algorithm

As the common migration algorithms, Kirchhoff migration is based on one-way-depth scalar wave equation, equation (2.7), whereas it is an integral solution. It yields three terms; the far-field term which is proportional to (1/r), and two other terms which are proportional to ($1/r^2$). Equation (2.7) can be written in Cartesian coordinate as:

$$\frac{\partial^2 P}{\partial x^2} + \frac{\partial^2 P}{\partial y^2} + \frac{\partial^2 P}{\partial z^2} = \frac{1}{V^2(x,y,z)} \frac{\partial^2 P}{\partial t^2} \tag{2.15}$$

Equation (2.15) gives the pressure wavefield P (x,y,z;t) propagating in a medium with velocity v (x,y,z) at a location (x,y,z) and at an instant of time t. The Kirchhoff solution is a mathematical statement of Huygens principle which states that the pressure disturbance at time $t+\Delta t$ is the superposition of the spherical waves generated by point sources at time t (Officer, 1958).

The discrete form of the integral solution to equation (2.15) as used in practical implementation of Kirchhoff migration is given by

$$P_{out} = \frac{\Delta x \Delta y}{4\pi} \sum_A \frac{\cos\theta}{vr} \frac{\partial}{\partial t} P_{in} \tag{2.16}$$

Where Δx and Δy are inline and crossline trace intervals, $P_{out} = P(x_{out}, y_{out}, z; \tau = 2z/z)$ is the output of migration using the input wave field $P_{in} = P(x_{in}, y_{in}, z=0; \tau = t - r/v)$ within an areal aperture A.

The Kirchhoff summation method requires computing nonzero-offset traveltimes through a 3-D, spatially varying velocity medium, as well as scaling and summation of the amplitudes along the computed traveltime trajectory based on the Kirchhoff integral solution to the scalar wave equation. Conceptually, the scaling of amplitudes before summation includes application of the obliquity factor cos θ, the spherical divergence factor $1/vr$, and the amplitude and phase corrections, $|\omega| \exp(i\pi/2)$, implied by the derivative operator $\partial P/\partial t$. Additionally, as for any migration, undersampling of the input data in x and y directions needs to be compensated for by a suitable anti aliasing filter (Yilmaz, 2001).

2.3 Depth Imaging

As explained previously, time migration is adequate for imaging the target that has velocity variation mild to moderate. Strong lateral velocity variation associated with structure-dependent (ex: diapiric structure) and structure-independent (ex: associated with facies changes). If one persistent to image the target with high lateral velocity variation, it would not yield a good quality and a correct image of a target below it. Thus, Strong lateral velocity variations associated with complex overburden structures require earth imaging in depth.

The other different thing between time migration and depth migration is the velocity used as an input of migration. Time migration and depth migration use root mean square (RMS) velocity and interval velocity, respectively. It is illustrated in Figure 2.8. In geophysical point of view, depth imaging has superiority in resolution, lateral and vertical positioning, as well as the accurate velocity and depth estimation (Fagin, 2002).

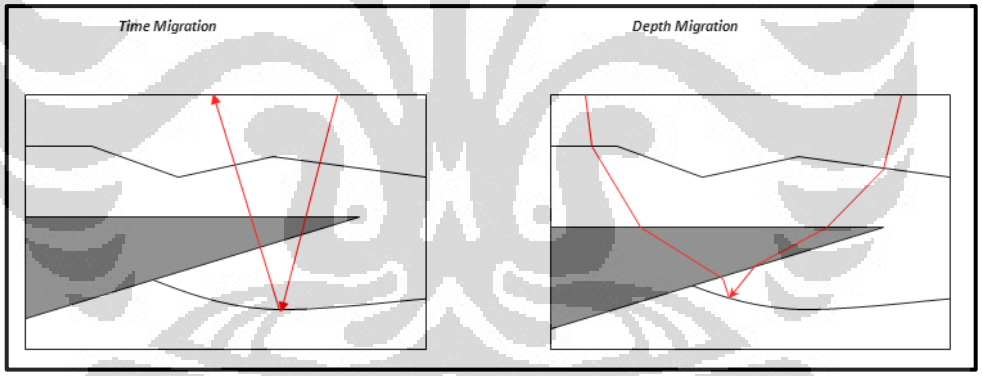

Figure 2.8 Ray path of RMS velocity in time migration (left) and interval velocity in depth migration (right) (Paradigm Geophysical Corp.,1996).

2.3.1 Initial Model Building

Several ways are available in determining velocity which is mostly based on ray theory and traveltime inversion of seismic data. And moveout forms in the gather are one of the bases for deriving velocities. The following are the ways to build initial velocity model (Yilmaz, 2001):

a) Dix transformation from RMS velocity,

b) Stacking velocity inversion,
c) Coherency inversion, and
d) Image gathers analysis of PSDM output.

- **Dix Conversion**

Dix (1955) derived equations for traveltime in the multilayered (flat) case by considering raypath bending. He discovered that, if small angle approximations were made, root mean square (RMS) velocity, when used in the moveout formula, closely predicts traveltime for any offset.Dix conversion is based on the formula

$$v_n = \sqrt{\frac{V_n^2\tau_n - V_{n-1}^2\tau_{n-1}}{\tau_n - \tau_{n-1}}} \qquad (2.17)$$

Where v_n is the interval velocity within the layerbounded by the $(n-1)$st layer boundary above and the nth layer boundary below, τn and $\tau n-1$ are the corresponding two-way zero-offset times, and Vn and V$n-1$ are the corresponding rms velocities.

There are 2 simplifications that makes the use of Dix conversion is limited. The first is raypath bending accounted for is limited due to the small angle that means the offset is small relative to depth. The second one is that the subsurface layers are flat. Levin, 1971, developed formula to adjust Dix values to account for dip, and the formula is

$$V_{nmo} * \text{cosine (dip)} = V_{rms} \qquad (2.18)$$

- **Coherency Inversion**

Landa and Koren (1971) presented the coherency inversion method in order to estimate the interval velocity values. Coherency inversion is one of the model-based techniques that model the overlying, previously established, structure to predict these effects. It uses raytracing to derive a family of moveout curves for a range of tested interval velocities. In this method, interval velocity is identified whose modeled moveout curve best matches coherent reflections over

some user-defined time window within the gather. Figure 2.9 shows the work of coherency inversion technique.

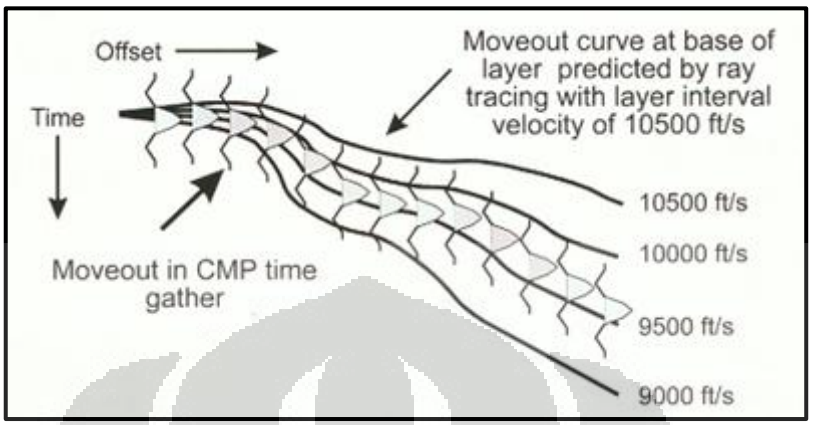

Figure 2.9 Coherency inversion technique works by calculating semblance along model-based trajectories (Fagin, 2002).

In estimating layer velocities, the coherency inversion requires CMP gathers at analysis location and horizon times picked. The coherency inversion is performed layer by layer starting from the top layer, it is referred as layer stripping method. In addition, the estimated velocity in this method is local which is independent of data away from the analysis location.

2.3.2 Model Refinement

- **Residual Moveout Analysis**

Image gathers as the result of initial model building can be used to update the initial velocity-depth model. Following the normal moveout correction of the CMP gather using this velocity function, events should look flat if the velocity function had been picked correctly. If the picking was done incorrectly, then you would observe events with residual moveout.

Analogous to the conventional stacking velocity analysis, if the initial velocity-depth model has been estimated with sufficient accuracy, then the image gathers derived from prestack depth migration using this model should exhibit flat events associated with the layer boundaries included in the model. Any errors in layer velocities and/or reflector geometries, on the other hand, should give rise to

residual moveout along those events on the image gathers. In principle, this residual moveout can be determined and used for model updating.

The semblance spectrum has two quadrants that correspond to positive and negative residual moveout, or equivalently, to positive and negative depth errors. A flat event would yield a semblance peak that coincides with the vertical axis with zero depth error, whereas an event with residual moveout would yield a semblance peak situated either in the left or right quadrant depending on the sign of the depth error. Much like picking a velocity function from a conventional stacking velocity semblance spectrum, a vertical function that represents the depth-dependent residual moveout can be picked from the semblance spectrum. This function can then be used to correct for the residual moveout (Yilmaz, 2001). Figure 2.10 depicts once the residual moveout overcorrected and undercorrected.

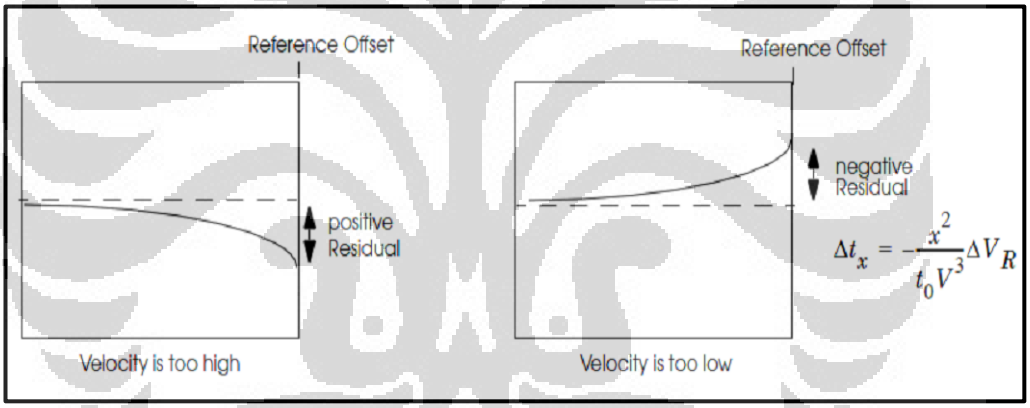

Figure 2.10 Positive residual moveout (right) and negative residual move out (left)

- **Reflection Tomography**

Both velocity and depth model can be updated in order to obtain the correct model as input of PSDM. The reflection traveltime tomography is one of the methods to update those models. Tomographic principle is to convert depth error to time error. Reflection traveltime tomography is based on perturbing the initial model parameters by a small amount and then matching the change in traveltimes to the traveltime measurements made from residual moveout analysis of image gathers (Sherwood et al., 1986; Kosloff et al., 1996).

Tomographic principle is easily understood by considering a subsurface model contains a numbers of layers and the traveltime along the ray of a reflected event from N_L^{th} is given by the integral

$$t = \int_{ray} S_L \, dl \,, \tag{2.19}$$

with S_L (x,z) the medium slowness. If small perturbations (δS_L , δz_i) is considered in the slowness and vertical coordinates of the intersection points of the ray with interfaces respectively, the resulting change to first order in traveltime is given by Farra and Madariaga (1988)

$$\delta t = \int_{ray} \delta \, S_L \, dl + \sum_{i=1}^{2N_L-1} \Delta P_z^i \, \delta z_i \,, \tag{2.20}$$

ΔP_z^i is the change in the vertical slowness of the ray between points directly above and below the *i*th interface. The first term on the right-hand side of equation (2.20) also appears in conventional cell-based tomography. The second term is more subtle and represents the traveltime change resulting from movement of interfaces that changes the length of the traversed path in each of the layers.

In velocity-depth determination method, equation (2.20) is used in three important applications which are conversion of migration depth errors to time errors along CRP rays, a fast prestack migration method yielding output in windows centered about the reflecting horizons, and the calculation of the tomography matrix (Kosloff, 1996).

The time error is then used in the calculation of tomography matrix. Equation (2.20) indicates the correlation between the time error, model parameter, and new model parameter.

$$\Delta t_n' = \sum_{m=1}^{n} (z_m - z_{m-1}) \sec\theta_m \, \Delta s_m + \sum_{m=1}^{n} (s_m \cos\theta_m - s_{m+1} \cos\theta_{m+1}) \, \Delta z_m \tag{2.21}$$

Equation (2.22) is a matrix form for all the traveltime perturbation from equation (2.21).

$$\begin{pmatrix} \vdots \\ \vdots \\ \vdots \\ \Delta t_n' \\ \vdots \\ \vdots \\ \vdots \end{pmatrix} = (\cdots \quad Z_m \quad \cdots \quad S_m \quad \cdots) \begin{pmatrix} \vdots \\ \Delta s_m \\ \vdots \\ \Delta z_m \\ \vdots \end{pmatrix} \tag{2.22}$$

Where

$$Z_m = (z_m - z_{m-1}) \sec \theta_m \tag{2.23}$$

and

$$S_m = s_m \cos\theta_m - s_{m+1} \cos\theta_m. \tag{2.24}$$

Equation (2.22) can be written in compact matrix notation:

$$\Delta t' = L\, \Delta p \tag{2.25}$$

The tomography update Δp to the model parameters that comprise the changes in the slowness and depths to layer boundaries is given by generalized linear inversion (GLI) solution

$$\mathbf{\Delta p = (L^T L)^{-1} L^T \Delta t}, \tag{2.26}$$

where Δt denotes the column vector that represents the residual moveout times measured from the image gathers, L is a sparse matrix — its elements are in terms of the slowness and depth parameters associated with the initial model, and T denotes matrix transposition.

2.4 Seismic Anisotropy

The definition of anisotropy was stated by various experts. Sheriff, 2001, stated that a medium is transversely isotropic if its elastic properties do not change in any direction perpendicular to an axis of symmetry. The usual meaning of seismic anisotropy is variation of seismic velocity, which itself depends on the elastic properties of the medium, with the direction in which it is measured. Winterstein (1990) also defined anisotropy which a medium is anisotropic if its intrinsic elastic properties, measured at the same location, change with direction, and it is isotropic if its properties do not change with direction. Intrinsic properties of medium might be permeability, porosity, resistivity, and so forth. In 2002,

Thomsen defined that seismic anisotropy is defined to be the dependence of seismic velocity upon angle.

In sedimentary rock sequences, the anisotropy may be caused by preferred orientation of anisotropic mineral grains (such as in a massive shale formation), preferred orientation of the shapes of isotropic minerals (such as flat-lying platelets), preferred orientation of cracks (such as parallel cracks, or vertical cracks with no preferred azimuth), or thin bedding of isotropic or anisotropic layers (Thomsen, 1986).

There are 2 cases of seismic anisotropy which are vertical transverse isotropy and horizontal transverse isotropy. In vertical transverse isotropy, the velocities do not vary from one lateral direction to another, but vary from one direction to another on a vertical plane that coincides with a given lateral direction. Horizontal bedding and fracturing parallel to the bedding produce transverse isotropy. The illustration of wave propagation in VTI media is depicted in Figure 2.11.

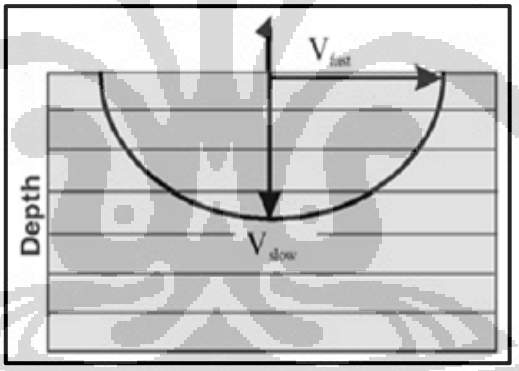

Figure 2.11 Wave propagation in VTI media (Lawton et al., 2001)

In the meantime, horizontal transverse isotropy, otherwise known as azimuthal anisotropy, for which velocities vary from one lateral direction to another. Fracturing in a direction other than the bedding direction gives rise to azimuthal anisotropy (Yilmaz, 2001). Figure 2.12 shows the wave propagation in HTI media.

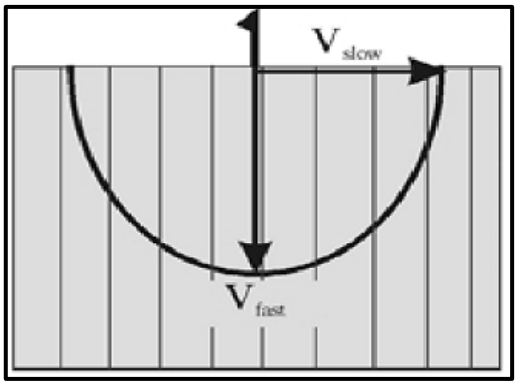

Figure 2.12 Wave propagation in HTI media (Lawton et al., 2001)

2.4.1 Types of Anisotropy

The generalized for of Hooke's law is the foundation of linear elastic theory. Hooke's law for general anisotropic, linear elastic solid states that the stress σ_{ij} is linearly proportional to the strain ε_{ij} as expressed by

$$\sigma_{ij} = c_{ijkl}\varepsilon_{ij} \tag{2.27}$$

in which summation is implied over the repeated subscripts *k* and *l*. The stiffness tensor, with elements c_{ijkl}, is a fourth-rank tensor obeying the laws of tensor transformation and has a total f eighty-one components (Mavko et al., 1998). The stiffness matrix, otherwise known as the elastic modulus matrix (Thomsen, 1986), that relates the stress components to the strain components is

$$\{c_{ij}\} = \begin{pmatrix} c_{11} & c_{12} & c_{13} & c_{14} & c_{15} & c_{16} \\ c_{21} & c_{22} & c_{23} & c_{24} & c_{25} & c_{26} \\ c_{31} & c_{32} & c_{33} & c_{34} & c_{35} & c_{36} \\ c_{41} & c_{42} & c_{43} & c_{44} & c_{45} & c_{46} \\ c_{51} & c_{52} & c_{53} & c_{54} & c_{55} & c_{56} \\ c_{61} & c_{62} & c_{63} & c_{64} & c_{65} & c_{66} \end{pmatrix} \tag{2.28}$$

The nonzero components of the more symmetric anisotropy classes commonly used in modeling rock properties are given below (Mavko et al., 1998).

Isotropic - two independent constants:

$$\begin{bmatrix} c_{11} & c_{12} & c_{12} & 0 & 0 & 0 \\ c_{12} & c_{11} & c_{12} & 0 & 0 & 0 \\ c_{12} & c_{12} & c_{11} & 0 & 0 & 0 \\ 0 & 0 & 0 & c_{44} & 0 & 0 \\ 0 & 0 & 0 & 0 & c_{44} & 0 \\ 0 & 0 & 0 & 0 & 0 & c_{44} \end{bmatrix}, c_{12} = c_{11} - 2c_{44} \tag{2.29}$$

The relations between the elements c and the Lame's parameters λ and μ of isotropic linear elasticity are

$$c_{11} = \lambda + 2\mu, c_{12} = \lambda, c_{44} = \mu \tag{2.30}$$

Cubic – three independent constants:

$$\begin{bmatrix} c_{11} & c_{12} & c_{12} & 0 & 0 & 0 \\ c_{12} & c_{11} & c_{12} & 0 & 0 & 0 \\ c_{12} & c_{12} & c_{11} & 0 & 0 & 0 \\ 0 & 0 & 0 & c_{44} & 0 & 0 \\ 0 & 0 & 0 & 0 & c_{44} & 0 \\ 0 & 0 & 0 & 0 & 0 & c_{44} \end{bmatrix} \tag{2.31}$$

Hexagonal or transversely isotropic - five independent constants:

$$\begin{bmatrix} c_{11} & c_{12} & c_{13} & 0 & 0 & 0 \\ c_{12} & c_{11} & c_{13} & 0 & 0 & 0 \\ c_{13} & c_{13} & c_{33} & 0 & 0 & 0 \\ 0 & 0 & 0 & c_{44} & 0 & 0 \\ 0 & 0 & 0 & 0 & c_{44} & 0 \\ 0 & 0 & 0 & 0 & 0 & c_{66} \end{bmatrix}, \tag{2.32}$$

where $c_{66} = \frac{1}{2}(c_{11} - c_{12})$

Orthorhombic - nine independent constants:

$$\begin{bmatrix} c_{11} & c_{12} & c_{13} & 0 & 0 & 0 \\ c_{12} & c_{22} & c_{23} & 0 & 0 & 0 \\ c_{13} & c_{13} & c_{33} & 0 & 0 & 0 \\ 0 & 0 & 0 & c_{44} & 0 & 0 \\ 0 & 0 & 0 & 0 & c_{55} & 0 \\ 0 & 0 & 0 & 0 & 0 & c_{66} \end{bmatrix} \tag{2.33}$$

2.4.2 Anisotropic Velocity Analysis

The P -wave phase velocity is given by (Thomsen, 1986)

$$\alpha(\theta) = \alpha_0(1 + \delta \sin^2 \theta \cos^2 \theta + \varepsilon \sin^4 \theta). \tag{2.34}$$

Note that the P -wave velocity depends on the anisotropy parameters δ and ε, but not on the parameter γ. In fact, the SV -wave velocity also depends only on δ and ε, while the SH-wave velocity depends only on γ.

In the special case of vertical incidence, θ = 0, equation (2.34) gives the vertical P -wave velocity, α_0.In the special case of horizontal incidence, θ = 90 degrees, equation (2.34) gives

$$\alpha_h = \alpha_0(1 + \varepsilon). \quad (2.35)$$

Solving for ε, we obtain

$$\varepsilon = \frac{\alpha_h - \alpha_0}{\alpha_0} \quad (2.36)$$

This equation provides a physical meaning for the Thomsen's parameter ε. Specifically, the parameter ε indicates the degree of anisotropic behavior of the rock, measured as the fractional difference between vertical P -wave velocity α_0 and the horizontal P -wave velocityα_h. Since for most rocks ε > 0, note that the horizontal P -wave velocity is greater than the vertical P –wave velocity.

The normal-moveout velocity $v_{NMO}(\varphi = 0)$, where φ is the dip angle, for a flat reflector in an anisotropic medium is given by Thomsen (1986)

$$v_{NMO}(0) = \alpha_0\sqrt{1 + 2\delta}. \quad (2.37)$$

In the special case of δ = 0, the moveout velocity is the same as the velocity of an isotropic medium represented by α_0.

The P -wave traveltime equation for a flat reflector in an anisotropic medium is given by Tsvankin and Thomsen (1994)

$$t^2 = t_0^2 + A_2x^2 + \frac{A_4x^4}{1+Ax^2} \quad (2.38)$$

Where *t* is the two-way time from source to reflector to receiver, t_0 is the two-way zero-offset time, *x* is the source-receiver offset, and A_2 and $A_4$are coefficients which are written below to acknowledge their complexity

$$A_2 = \frac{1}{\alpha_0^2(1+2\delta)} \quad (2.39)$$

$$A_4 = -\frac{2(\varepsilon-\delta)[1+2\delta(1-\beta_0^2/\alpha_0^2)^{-1}]}{t_0^2\alpha_0^4(1+2\delta)^4} \quad (2.40)$$

And

$$A = \frac{A_4}{\alpha_h^{-2}-A_2} \quad (2.41)$$

The travel time hyperbolic equation for a flat reflector in an isotropic medium is

$$t^2 = t_0^2 + \frac{x^2}{v_{NMO}^2} \quad (2.42)$$

For isotropic velocity analysis using equation (2.42), it needs to scan one parameter — the velocity v_{NMO}. For anisotropic velocity analysis using equation (2.38), note to do a multiparameter scan involving α_0, α_h, β_0, δ, and ε — an

impractical and unacceptable proposal. As a way to circumvent this insurmountable problem of a multiparameter scan in velocity analysis, Alkhalifah and Tsvankin (1995) define a new effective anisotropy parameter

$$\eta = \frac{\varepsilon - \delta}{1+2\delta} \tag{2.43}$$

By way of equations (2.35), (2.37), (2.43), (2.39), (2.40), and (2.41), and neglecting the effect of β_0, equation (2.38) takes a form that is suitable for practical implementation (Alkhalifah and Tsvankin, 1995)

$$t^2 = t_0^2 + \frac{x^2}{v_{NMO}^2} - \frac{2\eta x^4}{v_{NMO}^2[t_0^2 v_{NMO}^2 + (1+2\eta)x^2]} \tag{2.44}$$

where v_{NMO} is the flat-reflector moveout velocity. Equation (2.44) indicates that the travel time for a reflector in an anisotropic medium follows a non-hyperbolic trajectory.

Figure 2.13 shows the effect of hockey stick, which the gather is only analyzed according to equation (2.43) or second order equation. The effect of hockey stick is able to be corrected using equation (2.44) which involve the forth order equation.

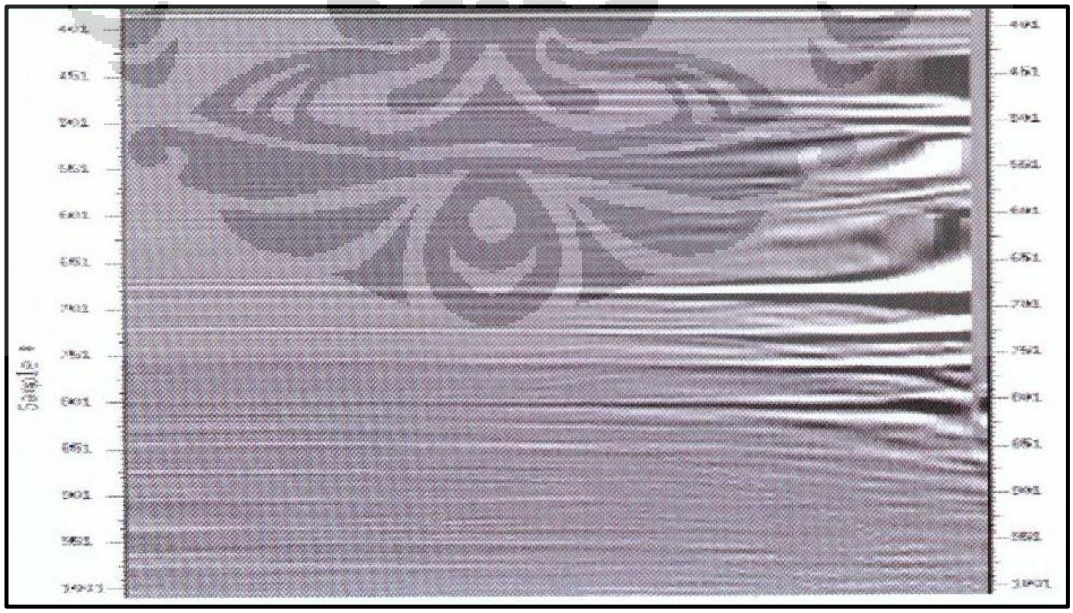

Figure 2. 13 Hockey stick effect at the far offset of gather

CHAPTER 3
METHODOLOGY

This chapter explains the workflow of data processing in both isotropic and anisotropic prestack depth migration. In Isotropic PSDM, the initial model is built by Dix conversion and coherency inversion while the refinement model uses RMO analysis and horizon-based tomography. Anisotropic PSDM also has the initial model building stage and model refinement stage which the models are anisotropic velocity and Thomsen's parameters, δ and ε. In addition, both the isotropy and the anisotropy steps are performed simultaneously.

3.1 Data Input

3.1.1 Seismic Data

Seismic data used are 2-D marine data, 1 line, that have minimum phase and normal polarity (SEG). Time gather, as input of anisotropic PSDM, have been processed prestack time migration whereas RMS velocity section is used as input velocity. The outputs of prestack time migration are prestack time migration (PSTM) section and time migrated gathers. Those acquired data are then used to build interval velocity model. However, only time gather and interval velocity model that processed as an input of both isotropic and anisotropic PSDM. The output of isotropic prestack depth migration are depth migrated gather as well as depth migrated section. These data output are then used as reference to analyze non-flat event in the depth gather in order to build the velocity refinement model.

In the step of anisotropic PSDM, the inputs used are time gather, anisotropic velocity model, δ and ε. The anisotropic velocity model is obtained by transforming final isotropic interval velocity and δ. Anisotropic parameter calculation is estimated by relationship of seismic horizons and well-markers.

3.1.2 Well Data

The location of 'wildcat' well is adequate close to the seismic line which the distance is about 169.47 m. In the well data, there is no provided information

of well-markers, it is then generated through sonic log and gamma-ray log. The information of artificial well marker is showed by the following table:

Table 3.1 Depth of well-marker

Assigned well markers	Depth (meter)
RI1	731.291
RI2	976.238
RI3	1139.670
RI4	1371.740

The well markers together with seismic horizons are used to calculate the anisotropy parameter, δ and ε.

3.2 Isotropic PSDM

Before performing isotropic prestack depth migration, several data such as prestack time migration (PSTM) section, RMS velocity section, and time migrated gathers are used in the process interval velocity-depth model building. The time gathers as the input of PSDM need to pass the pre-conditioning processes. After preconditioning, the data is expected have minimum noise to make the process of model building. However, the quality of those data input affect the process of building the velocity and layer structure model.

In this study, the process of defining initial velocity and layer structure model is using layer stripping method where the velocity and structural model is defined layer by layer. Coherency inversion is used to define the velocity layer prior to layer structure. Meanwhile, Dix conversion is used for the one upper layers and coherency inversion does the rest of layers.

Inaccurate velocity model in the initial stage still remains the velocity error. In order to diminish the error, the refinement stage should be taken to yield better interval velocity and depth model. Refinement stage contains of residual move-out (RMO) analysis and horizon-based tomography which used to deal the error in the near offset. The reflectors events in the near-offset gather would be flat once the appropriate velocity used to make it flat. Residual move-out analysis

and tomography is performed iteratively to yield the zero move-out error in the depth gather that also represent appropriate velocity-depth model. In determining the isotropic velocity, the velocity model building is constrained just for the reflector at the near-offset. Hence, the gather is muted in 30 degree as long as isotropic PSDM process.

The input data of isotropic depth migration are time gather and interval velocity model, while the output data of isotropic prestack depth migration are depth gathers and depth migrated section.

3.2.1 Initial Model Building

As explained previously, layer stripping method is used in building initial model. It is solving the depth imaging conundrum, yet this method is still not perfect. Layer stripping itself has a limitation which the error of each layer will be accumulated. Inaccurate velocity on the upper layer will generates error that will affect the next lower layers. It means that the deeper horizon or layer will have bigger error.

In order to diminish the error accumulation, the model of every layer should be defined properly. In this stage, horizon interpretation and Dix conversion as well as coherency inversion need to be performed with high fidelity. Figure 3.1 shows the workflow of building initial model.

- **Horizon Interpretation**

In the first step of initial model building, horizons need to be created to distinguish one formation to another. In order to pick the right horizons in time migrated gathers, it needs to correlate the strong reflection event in the stack section to well data. It leads to put up the appropriate velocity to each horizon.

This marine data have polarity normal as well as minimum phase (SEG standard). By that information, it is easily identified that the first horizon is picked on “trough to peak” because the boundary between sea water and first layer have

positive coefficient reflection. Picking on 'trough to peak' is also followed to the next layers below. Figure 3.2 shows the first horizon in the seismic section.

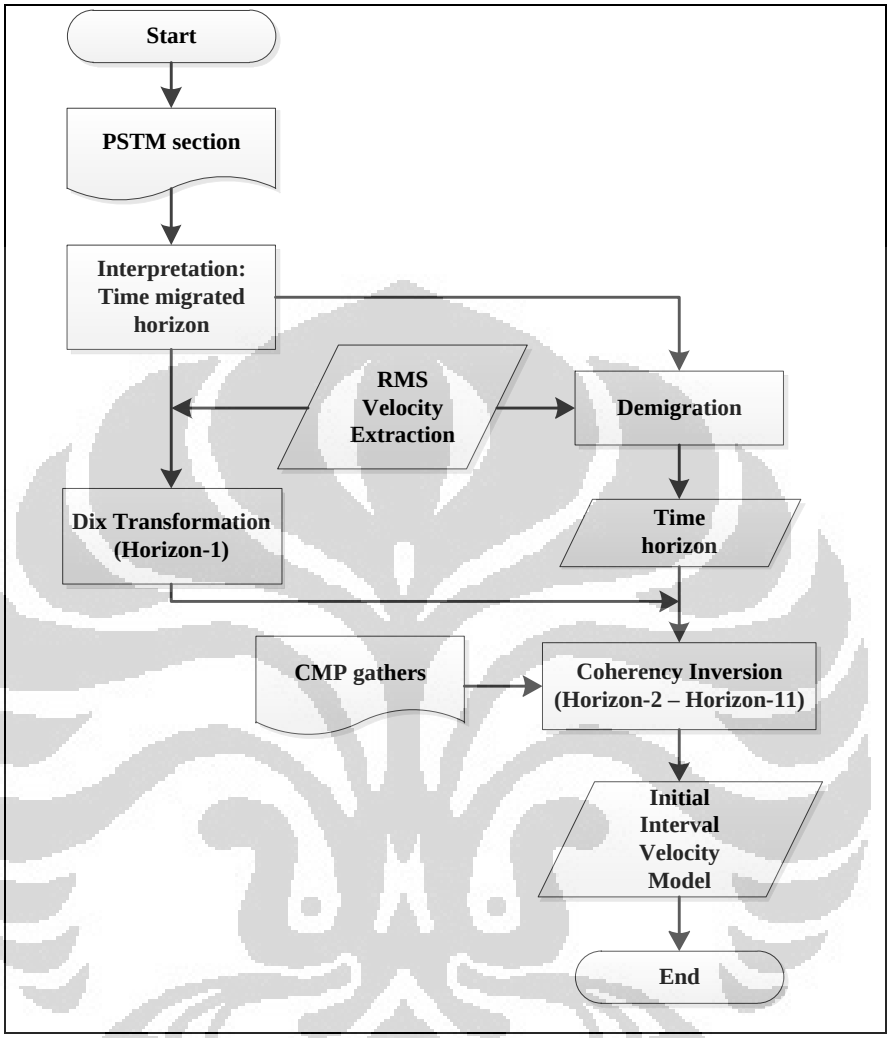

Figure 3.1 Flowchart of initial model building

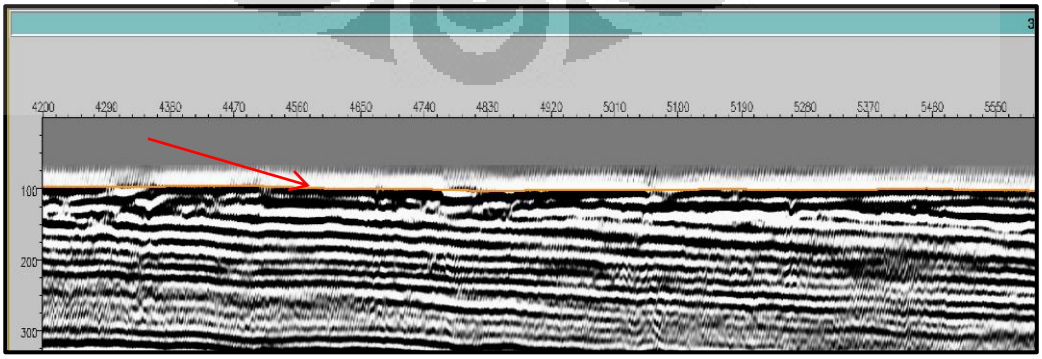

Figure 3.2 First horizon in time migrated domain

- **Dix conversion**

Dix conversion is only used for the first top layer due to the next layer below is not fulfill the requirement of this transformation. The first top layer is a boundary between sea water column and bedrock which relatively flat. And the next layer below has adequate dipping structure. It might generate unreliable interval velocity, large error, if Dix conversion applied for the next lower layer.

Dix conversion needs RMS velocity value as input to generate the interval velocity. In the Dix conversion, the RMS velocity value of all horizons picked in time migrated section can be directly extracted from the RMS velocity section. Figure 3.3 shows the RMS velocity extracted. As can be seen, the value of RMS velocity is higher when the horizon is deeper.

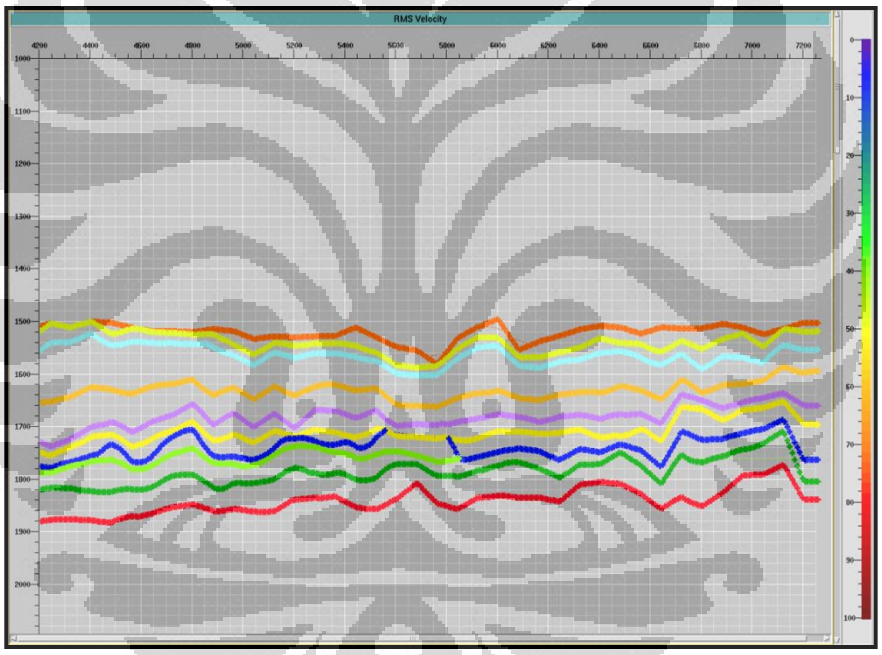

Figure 3.3 RMS velocity extraction

After the RMS velocity of each horizon extracted, it can be directly transformed to interval velocity, only for the first top horizon. The transformation is according to equation 2.17. The first interval velocity layer is used to define the layer structure. Then, performing image-ray depth conversion of the time horizons interpreted from the time migrated section to generate the depth. The result of Dix conversion is depicted in Figure 3.4.

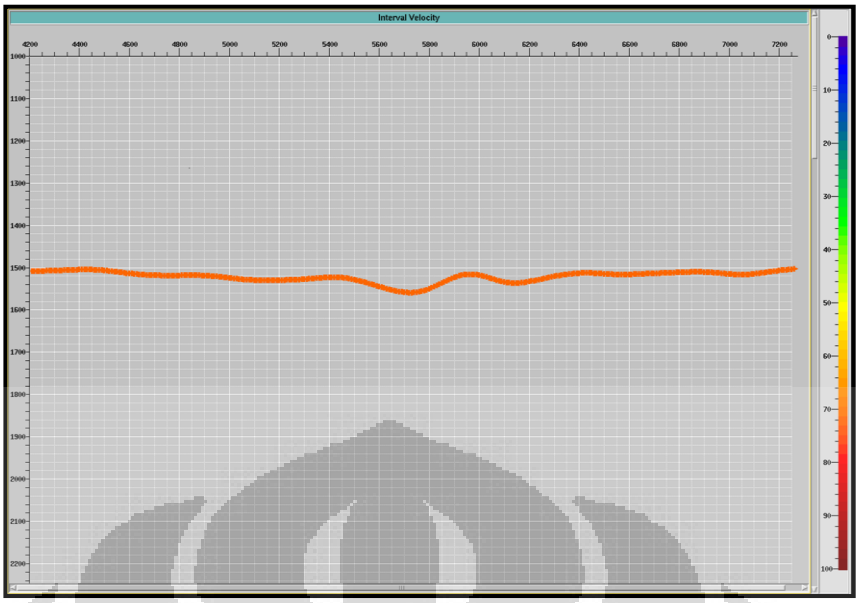

Figure 3.4 Interval velocity transformed by Dix formula

- **Coherency Inversion method**

Due to the limitation of Dix conversion, coherency inversion takes the main part in initial model building. The coherency inversion, which is based on ray tracing method, is used to define the velocity and layer structure model for horizon-2 until horizon-10.

In contrast to Dix conversion, the horizon in coherency inversion process is migrated from time unmigrated domain. Thus, all horizons in time migrated domain is firstly demigrated to unmigrated time domain which using RMS velocity as input of demigration. Figure 3.5 shows the unmigrated horizons which obviously seen the presence of intersection in horizon-7.

As explained previously, initial model building is using layer-stripping method whereby the velocity and layer structure is defined layer-by-layer. It means R2 is started firstly before moving to the next layer below as well as the velocity model is defined prior to layer structure model. The velocity model is obtained by picking velocity where semblance as guidance to flatten the CMP gather. The appropriate velocity picked yields the flat gather. If the velocity picked is too fast rather than appropriate velocity, the gather will be

undercorrected. Conversely, the reflector event is overcorrected if the velocity is too slow.

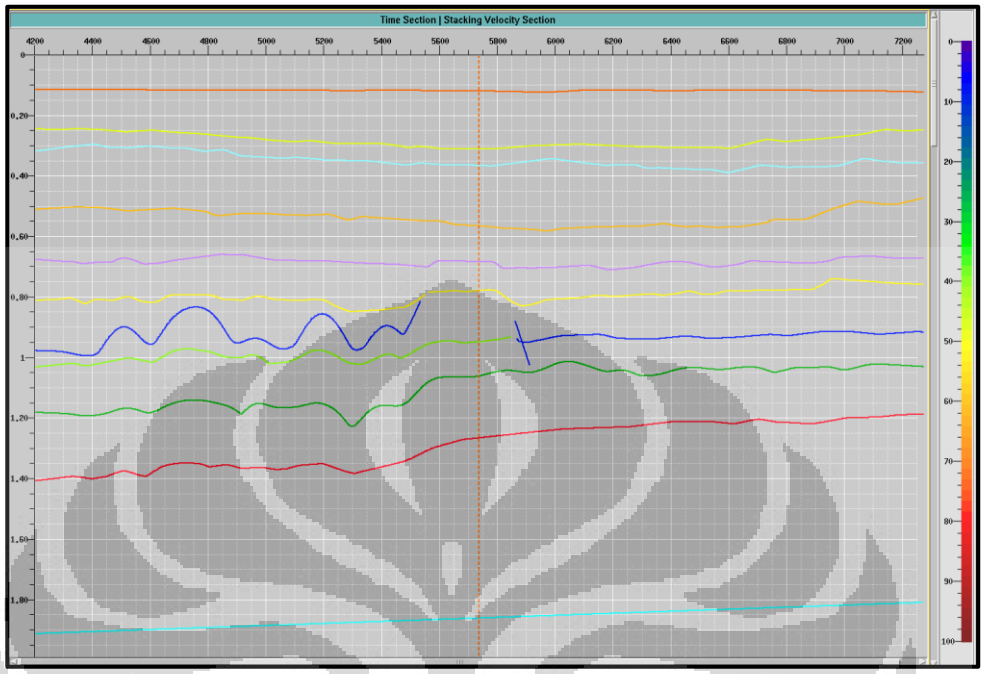

Figure 3.5 Velocity horizon in time unmigrated domain

Figure 3.6 portrays the process of picking interval velocity. On the left below part, that is the semblance where the velocity picked. And the right side of the picture, there is a CMP gather that as guidance whether the velocity picked is right or not. The interval velocity picked is involved in Δt calculation.

After velocity along a horizon defined, the next step is to build layer structure model. Layer structure can be easily created after migrating the horizon from time unmigrated. Once the one horizon completed, the next lower horizon can be performed coherency inversion with the same way as before.

The end results of initial model building are the interval velocity model and the layer structure model. Figure 3.7 shows the interval velocity section with the layer structure in all horizons. The results are then used as inputs in the step of migration.

In the migration stage, time gather and velocity section are used as inputs in isotropic prestack depth migration. Kirchhoff algorithm is selected in the

migration process whereas the wavefront method is used in traveltime calculation. Figure 3.8 shows the parameter of Kirchhoff migration.

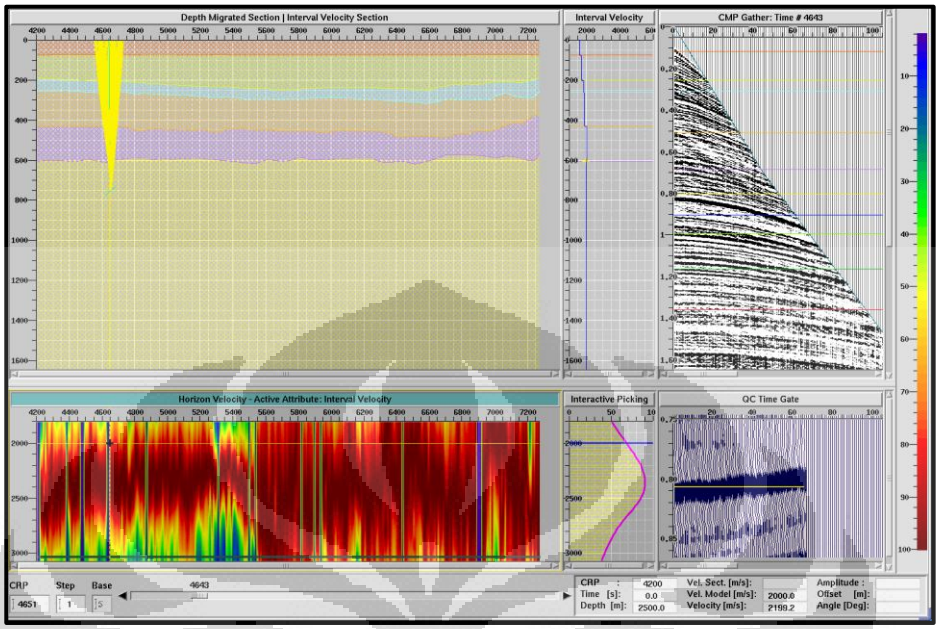

Figure 3.6 The process of coherency inversion on the horizon-7 layer

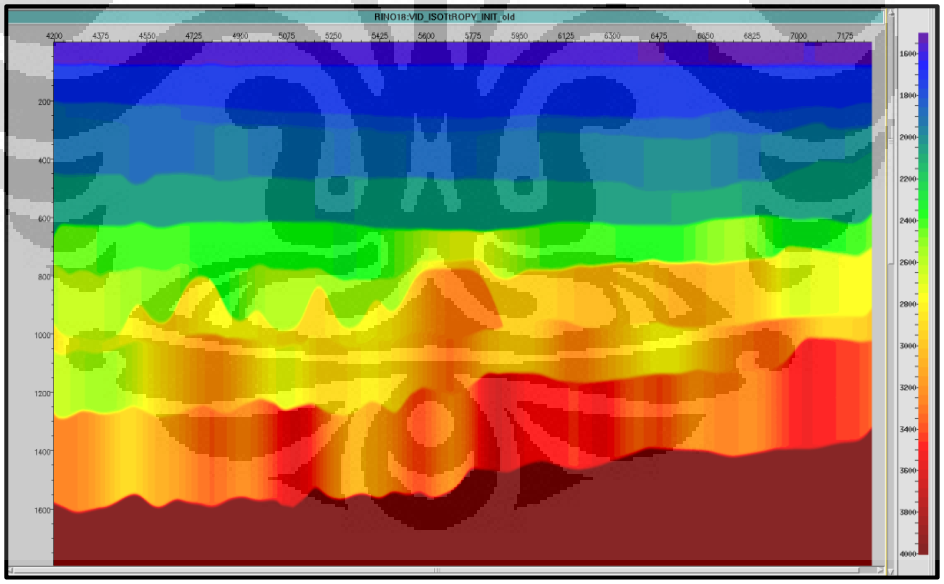

Figure 3.7 Initial interval velocity section

The number of migration parameters in Kirchhoff needs to be selected properly. Aperture width is the critical parameter that drives the quality of migration. Aperture calculation is according to the equation (3.1) whereas depend

upon the maximum depth and CMP interval of seismic data. In this study, maximum depth and interval CMP is 2000 meter and 6.25 meter, respectively.

Meanwhile, the other parameters are also needed to be considered such as travel time method and amplitude correction method. The travel time is calculated based on maximum energy of P-wave and geometrical spreading is selected in amplitude correction.

$$\text{Number of CMPs} = \text{Aperture} = \frac{2 \text{ x Max Depth x } 0.75}{\text{CMP Interval}} \qquad (3.1)$$

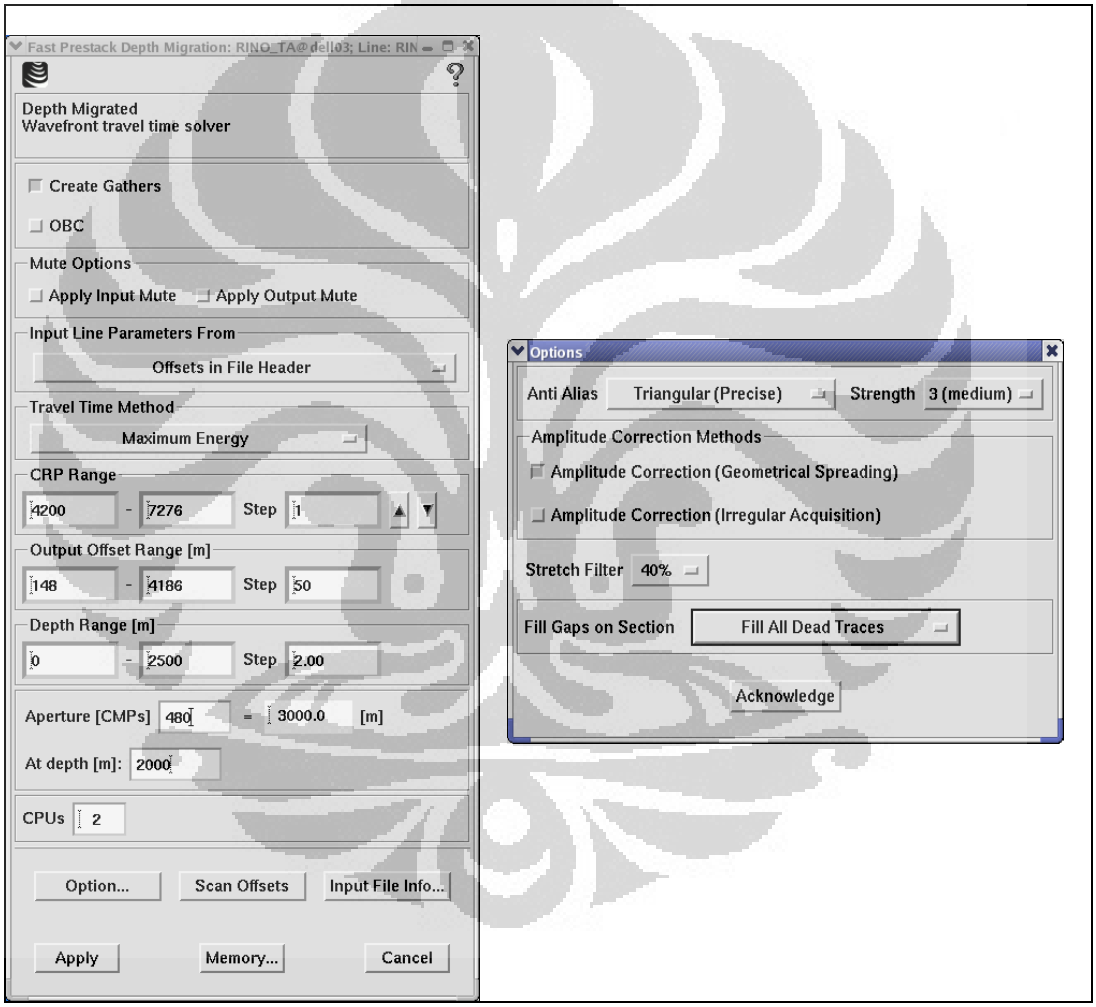

Figure 3.8 Migration parameter

The results of isotropic prestack depth migration, seismic depth migrated section and depth migrated gather, is then analyzed whether the result is proper or

not. The flatten gather is a parameter that want to be achieved. If the gather is already flat, it can be directly continued to anisotropic PSDM stage. As showed in Figure 3.9, the result of initial isotropic PSDM in this study still conducts non-flat reflector at the near-offset due to inaccurate interval input used in PSDM.

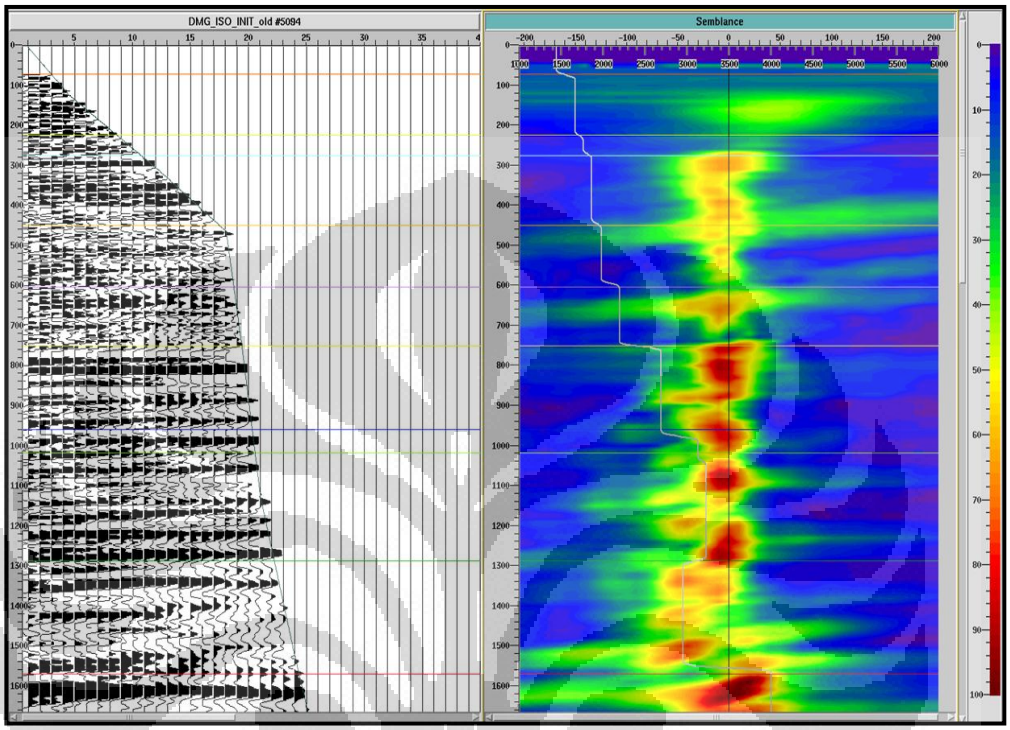

Figure 3.9 Depth gather as the result of initial isotropic PSDM

3.2.2 Model Refinement

The result of isotropic PSDM still yields non-flat reflector in depth migrated gather. It indicates the velocity used in initial model is slightly inaccurate. Fortunately, there are several available ways to refine the initial interval velocity. Residual moveout analysis and horizon-based tomography are the ways to solve the obstacle to obtain the appropriate interval velocity.

Figure 3.10 shows the workflow of isotropic model refinement. The process of model refinement might be performed simultaneously until the optimum interval velocity model achieved. On the first step of refining model, the

seismic depth migrated section as the output of the first isotropic PSDM needs to be re-interpreted.

The horizons picked should be consistence with the event reflector that picked in time migrated section. It is then continued with picking residual velocity and the picked residual velocity is used as input in horizon-based tomography to build new interval velocity and layer structure model. In order to prove whether the new interval velocity is proper or not, the process of isotropic PSDM is taken. The output of isotropic PSDM in refinement stage is then analyzed properly whether the depth migrated gather is already flat or not. If the gather is flat, the next step is anisotropic PSDM. Conversely, if the gather is not flat, it returns to the first step of model refinement. Thus, the process of model refinement is iterative process whereby in this work there are 3 iterative processes.

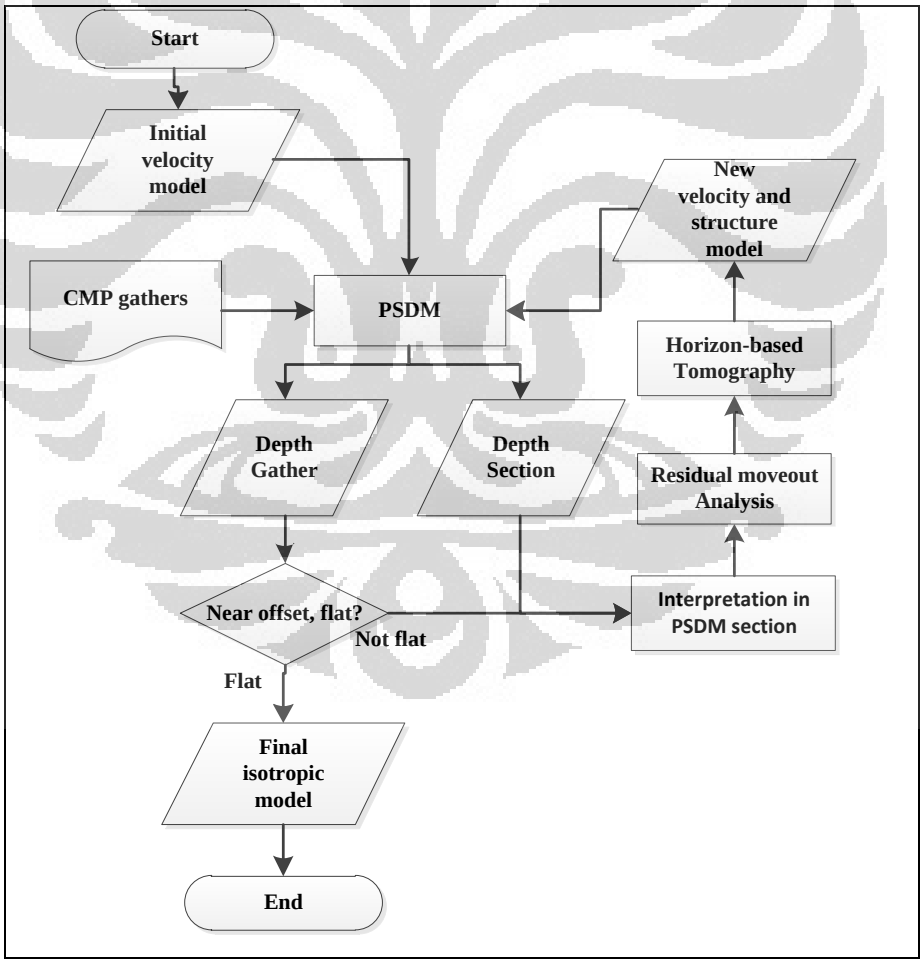

Figure 3.10 Flowchart of model refinement

- **Residual Move-out Analysis**

Residual move-out analysis is carried out once the interval velocity is still inaccurate. It is not re-defining the new interval velocity, yet only diminishing the error of initial interval velocity. It is the process of adding or reducing the value of initial interval velocity. By that reason, residual move-out analysis really depends upon the initial model. That's why the initial model is completely important.

In order to pick the residual interval velocity, residual RMS semblance needs to be created. The residual semblance provides information regarding the appropriate interval velocity that will be picked along horizon. As showed in Figure 3.11, the trend of dominant red color on the bottom of the picture mostly indicates the zone of the correct velocity to flatten the gather. Although the proper velocity is not always presence in the red color zone, the key guidance to pick the right velocity is by looking the gather. In contrast to coherency inversion, the depth migrated gather can be analyzed directly in the process of picking residual moveout. The depth migrated gather change suddenly once the semblance picked. The stage of picking residual velocity is processed along horizon while increment is 50 CMP's.

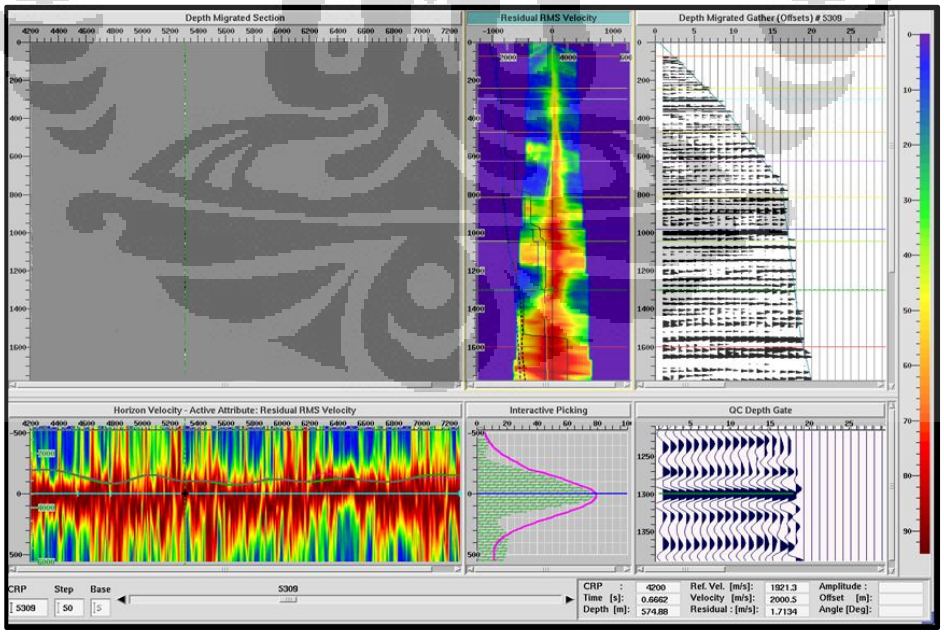

Figure 3.11 Picking residual move out on horizon-9

- **Horizon-Based Tomography**

After picking residual velocity finished, it is then used as an input in the tomography process. In this study, the kind of tomography used is horizon-based tomography. Basically, it is using the picking result of RMO analysis and new horizon interpretation after migration of initial PSDM as input. Then, it calculates the depth-velocity error of the previous velocity-depth model and define the new velocity-depth model afterwards. Figure 3.12 and figure 3.13 shows the parameter of horizon based tomography and the final isotropic interval velocity section (refinement-3), respectively.

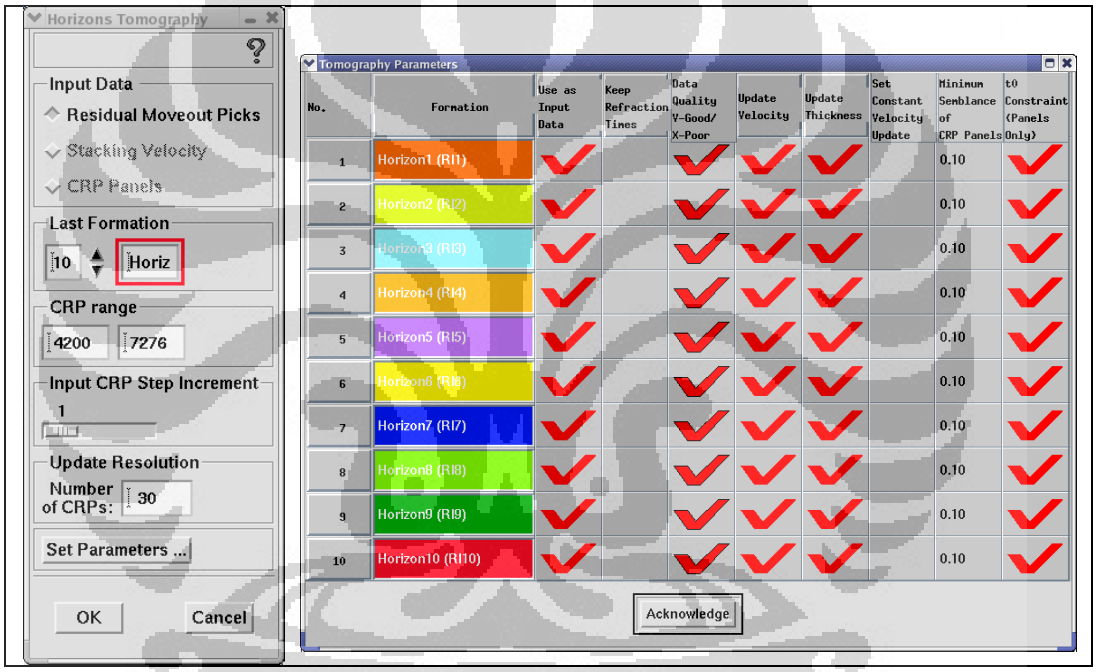

Figure 3. 12 Horizon-based tomography

After the process of horizon-based tomography finished, the next step is doing isotropic PSDM whereas the Kirchhoff migration performed and the gather stacked afterwards. The optimal velocity model is obtained after refinement-3 performed. The optimal isotropic interval velocity section is turning out the flatten gather in the near-offset and can be continued to anisotropic stage.

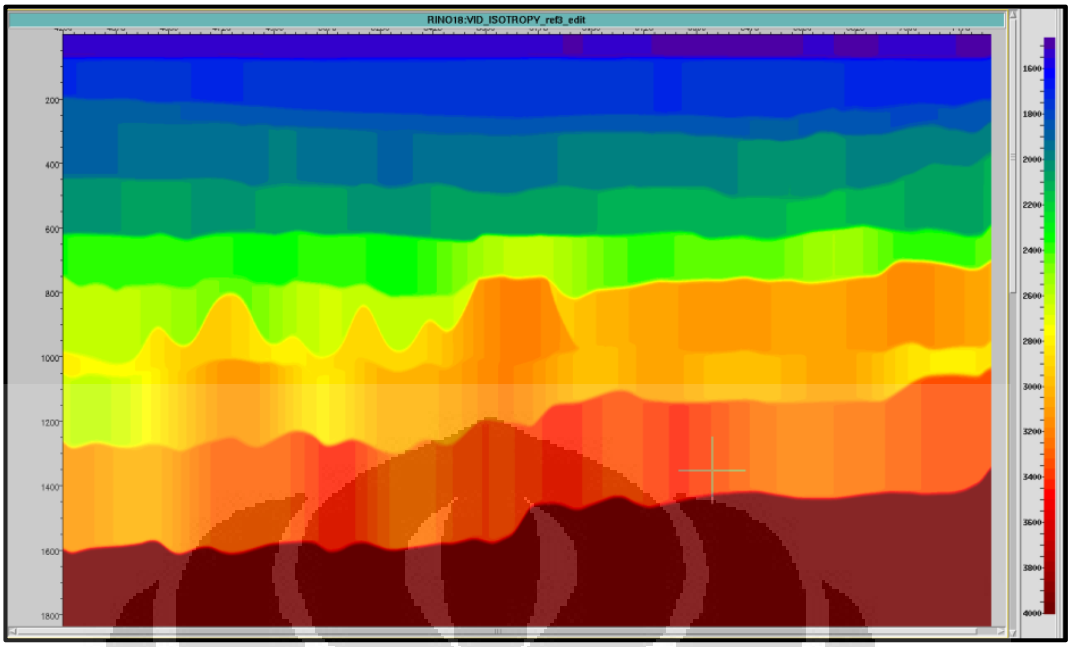

Figure 3.13 Final isotropic interval velocity section (refinemet-3)

3.3 Anisotropic PSDM

Different with isotropic PSDM, the analysis of depth gather is not limited in mute 30 degree, yet until far-offset. Within the process of anisotropic PSDM, isotropic interval velocity is transformed to anisotropic velocity which the anisotropic parameter δ involved into the transformation. Anisotropic PSDM itself has 4 input parameters which are time gather, anisotropic interval velocity, δ and ε. Figure 3.14 shows the flowchart of anisotropic PSDM. It is divided into 2 main stages which are initial model building and model refinement. Model refinement is performed simultaneously in order to obtain optimum anisotropic parameters.

3.3.1 Initial Anisotropic Model Building

- **Initial Anisotropic Parameter Building**

Anisotropic parameters, δ and ε, should be determined first before starting to build anisotropic velocity. δ indicates the degree of anisotropy in near-vertical

direction. δ is calculated according to equation (3.2) whereby well markers and seismic horizons are involved.

$$\delta_n = \frac{1}{2}\left[\left(\frac{v_0^I}{v_0^A}\right)^2 - 1\right] = \frac{1}{2}\left[\left(\frac{\Delta Z^I}{\Delta Z^A}\right)^2 - 1\right] \quad (3.2)$$

ΔZ^I = Isotropy layer thickness (measured from the structural model and seismic velocity)

ΔZ^A = Anisotropy layer thickness (measured from the well time-depth pairs log between T1 and T2).

δ_n= the degree of anisotropy in near vertical direction for horizon-n (n=1,2,3,..,11)

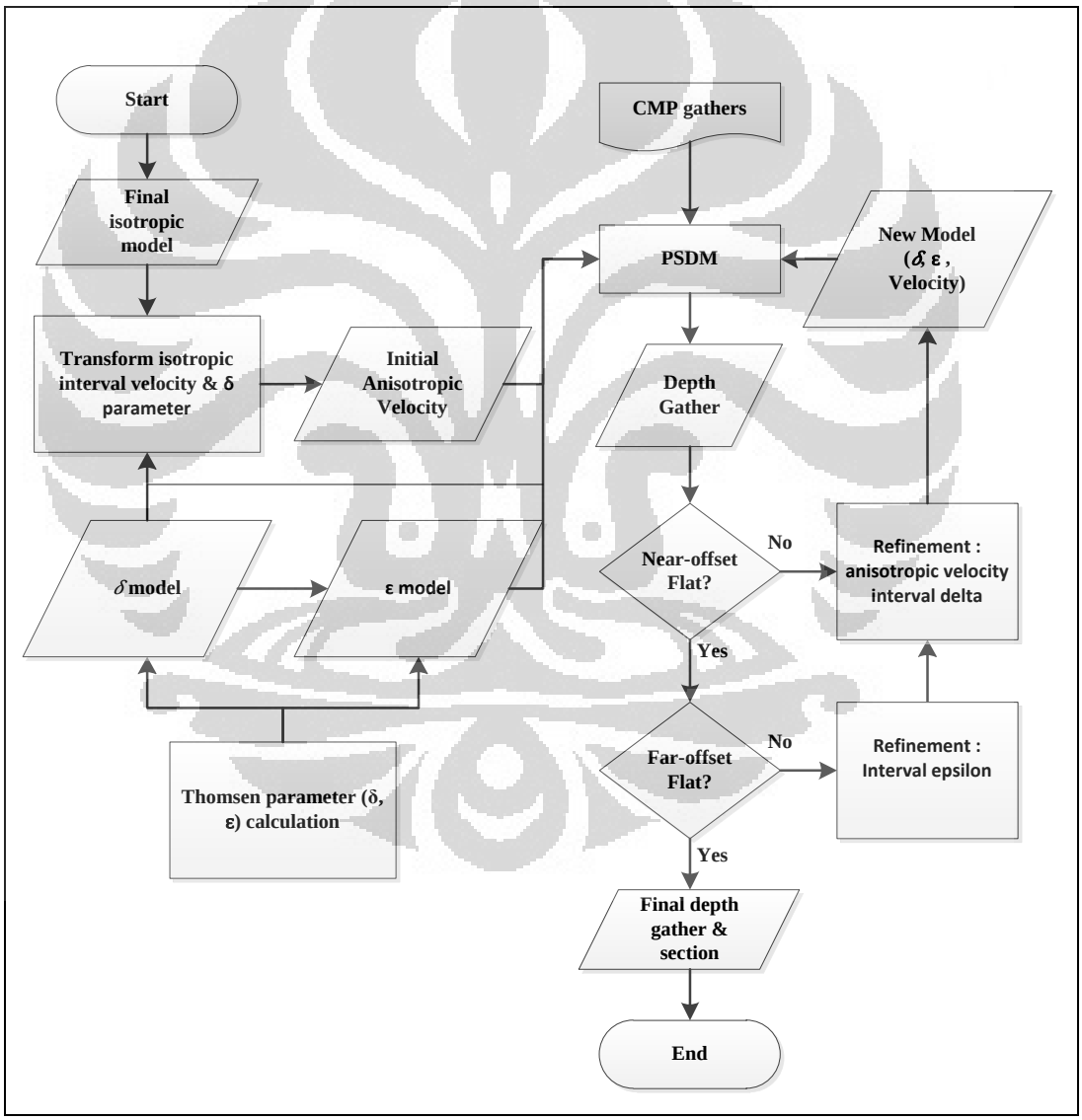

Figure 3.14 Flowchart of anisotropic PSDM

Table 3.2 shows the result of δ calculation whereas based on equation (3.2). The distinction of seismic horizons and well-markers contribute to the δ value. The well-marker started from horizon-6 until horizon-10. Since the horizon-9 is not crossing the well position, δ value of its horizon set as horizon-8. In addition, the δ of horizon-1 until horizon-5 is set equal to horizon-6.

Table 3.2 δ calculation

Seismic horizon	Depth (m)	Well-marker	Depth (m)	ΔZi	ΔZa	δ
Horizon-1						
Horizon-2						
Horizon-3						
Horizon-4						
Horizon-5						
Horizon-6	761.463	RI-1	731.286	761.463	731.286	0.04212
Horizon-7	988.637	RI-2	976.117	227.174	244.831	-0.05952
Horizon-8						
Horizon-9	1139.590	RI-3	1139.770	150.953	163.653	-0.07459
Horizon-10	1433.533	RI-4	1371.370	293.943	231.600	0.30541
Horizon-11						

The value of δ is then used to build the δ interval section. Figure 3.15 depicts the initial δ section. It can be seen that layer-9 has the biggest δ parameter. Meanwhile, the epsilon is firstly set up equal to 0 and the section is showed in figure 3.16.

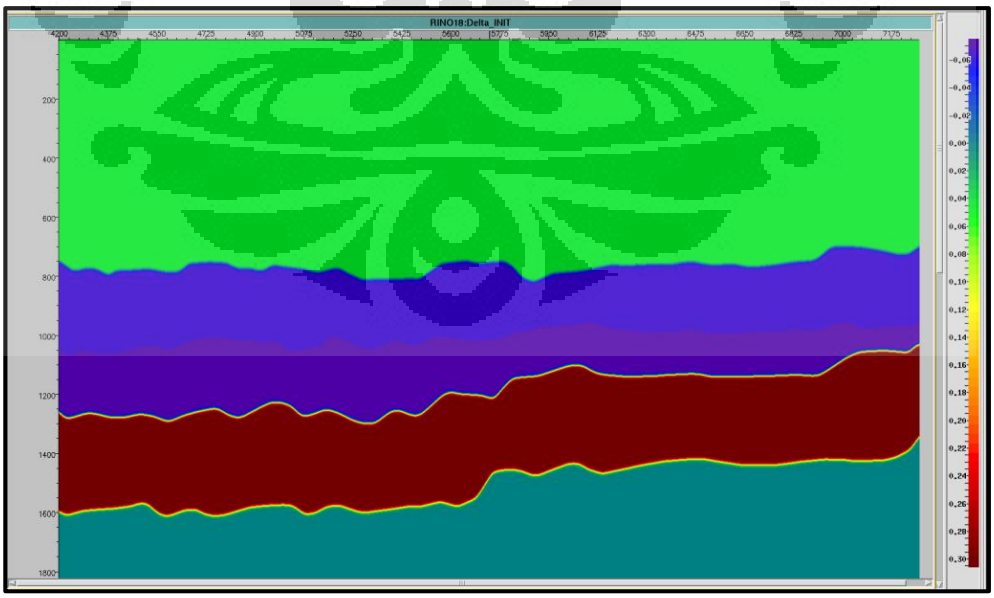

Figure 3.15 Initial Delta, δ, Section

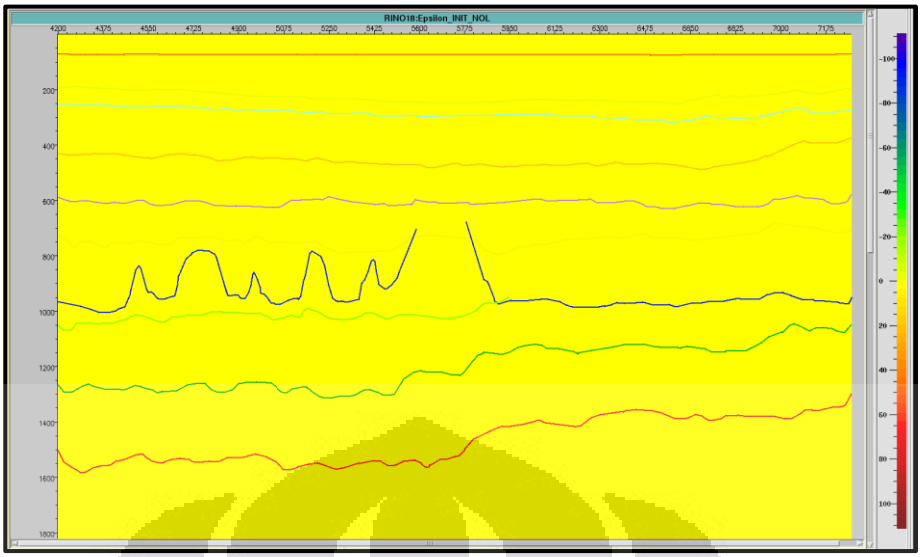

Figure 3.16 Initial Epsilon, ε, Section

- **Initial Anisotropic Velocity Model Building**

After initial δ obtained, isotropic velocity (V_0) is scaled down to anisotropy according to equation (3.3) which is the transformation normal-moveout velocity in anisotropic medium. Besides isotropic velocity, δ is involved into the transformation.

$$V_0^a = \frac{V_0}{\sqrt{1+2\delta}} \tag{3.3}$$

Figure 3.17 shows the result of initial anisotropic velocity. It can be seen in the horizon-6 and horizon-10, the anisotropic velocity is getting slower than isotropic velocity while δ is positive. In contrast, the horizon-7 and horizon-9 has negative value, hence the anisotropic velocity on those horizons are getting higher.

Once the anisotropic velocity section obtained, the process of prestack depth migration is performed. In anisotropic depth migration, Kirchhoff algorithm is selected with the same migration parameter as isotropic migration does. In addition, the inputs of anisotropic depth migration are time gather, anisotropic velocity section, δ section, and ε section. The depth gather of anisotropic PSDM,

which ε is set zero, depicted in figure 3.18. The hockey stick effect still presence due to the epsilon value is set on 0 (zero) value.

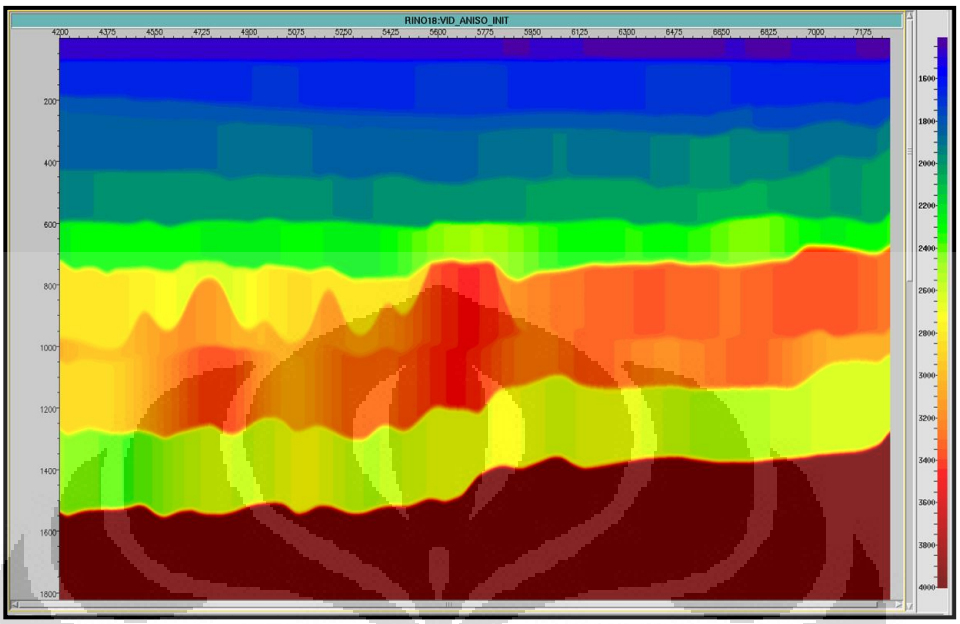

Figure 3.17 Initial anisotropic velocity section

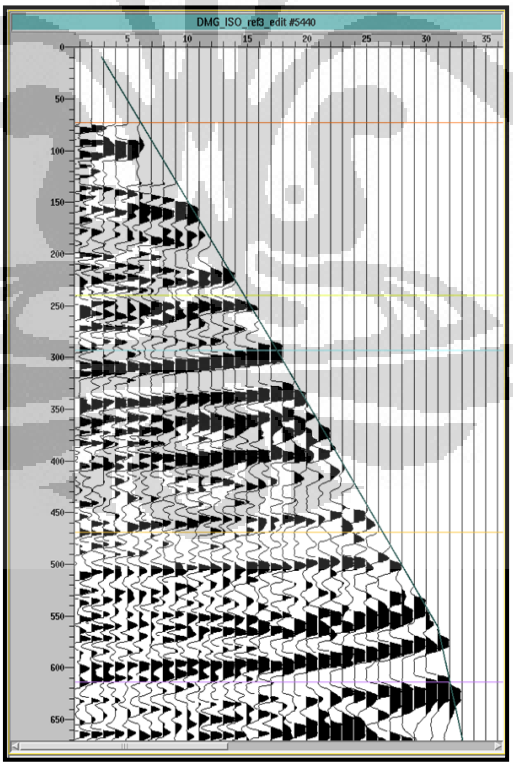

Figure 3.18 Depth gather as the result of initial anisotropic PSDM

3.3.2 Anisotropic Model Refinement

In the stage of model refinement is performed to refine the value of epsilon, δ and anisotropic velocity. The refinement process might be performed simultaneously until the optimum result, flatten gather until far-offset, achieved.

- **Anisotropic Velocity Refinement**

Anisotropic interval velocity might be refined while the gather in the near-offset haven't flat yet due to the influence of anisotropic parameter. As a solution, residual moveout analysis for the near-offset can be performed by picking the residual anisotropic interval velocity. Then, global tomography (VTI) is performed in order to update the anisotropic interval velocity. And the picked residual moveout is used as an input of anisotropic global tomography. Figure 3.19 shows the differences between anisotropic velocity section refinement-1 and final anisotropic velocity section refinement-2. The anisotropic velocity passes 2 times refinement process.

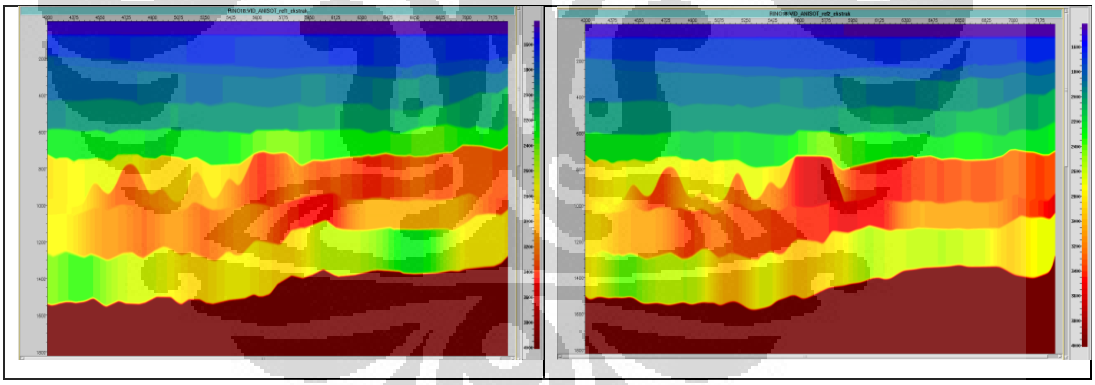

Figure 3.19 Anisotropic velocity section refinement-1 (left) and final anisotropic velocity section refinement-2 (right)

- **Anisotropic Parameter Refinement**

Depth gather of initial anisotropic PSDM still conducts the presence of hockey stick effect. It is caused the initial value of epsilon for each layer is set

equal to 0 (zero) value. Epsilon describes the fractional difference of P-wave velocities in the vertical and horizontal direction (Mavko et al., 1998). Thus, epsilon refinement needs to be performed in order to flatten the depth gather at the far-offset. It might be performed by picking residual interval epsilon. Figure 3.20 shows the depth gather where the interval epsilon semblance before picked and after picked. It can be obviously seen that the gather at the far-offset is flat once the right epsilon value picked. Thomsen (1986), based on his experiment, said that there is no negative epsilon. It means that the reflector event of depth gather can be only pushed down and cannot be pulled up.

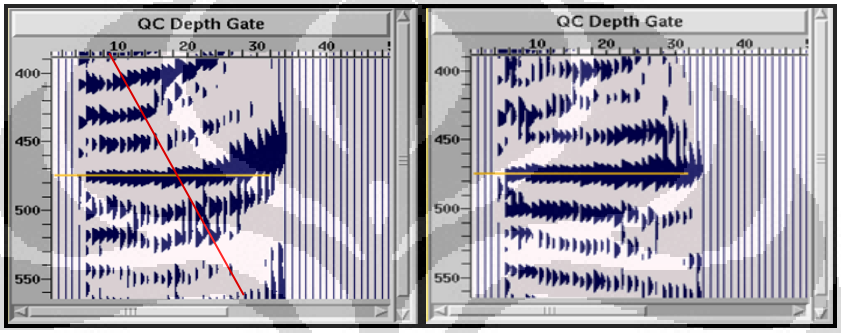

Figure 3.20 Gather before epsilon picked (left) and after epsilon picked (right)

The product of epsilon refinement is interval epsilon section which shown in Figure 3.21, refinement-1 and refinement-2. It clearly shows the distinction between initial epsilon section and final epsilon section. As the result, the interval epsilon affects the P-wave velocity variation laterally.

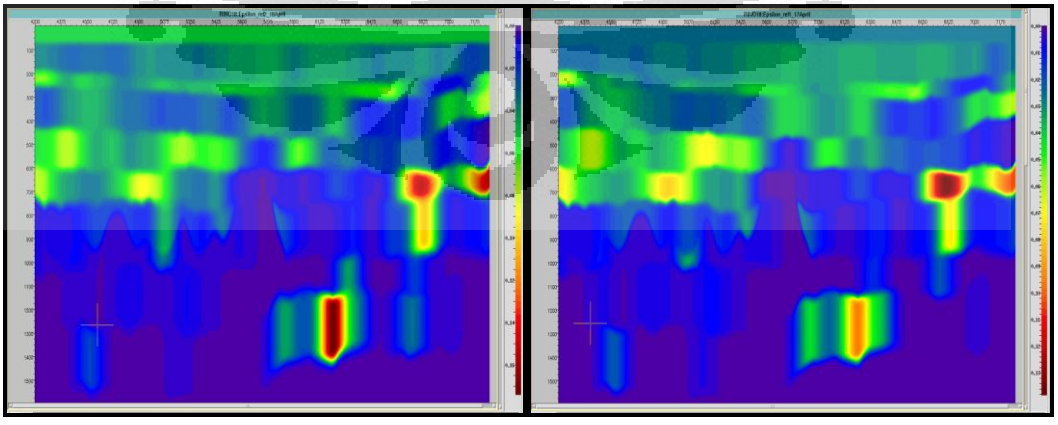

Figure 3.21 Epsilon section refinement-1 (left) and final epsilon section refinement-2 (right)

CHAPTER 4
RESULTS AND ANALYSIS

4.1 Isotropic PSDM

In the initial model building, Dix conversion and coherency inversion is used to determine the initial model. Dix conversion is only possible to be used in the first layer which is the seafloor, while coherency inversion defines the rest of layers. Coherency inversion becomes difficult when the gather picked not clearly shows the flat reflector and semblance not shows the pattern.

In practice, the semblance of horizon-1 until horizon-6 show the excellent pattern and make the velocity picking process easily made. In contrast, it is somewhat difficult to define the appropriate velocity in the horizon-7 until the last horizon, horizon-10. Once the gather is hard to give a clue about the right velocity picked, semblance offers assistance on it. Semblance is used as a guidance to pick the right velocity to the gather. The example of coherency inversion in this study is depicted in Figure 4.1. Mostly, the gather condition affects the pattern of semblance, meanwhile the gather condition is influenced by structural geology and the physical properties of the layer.

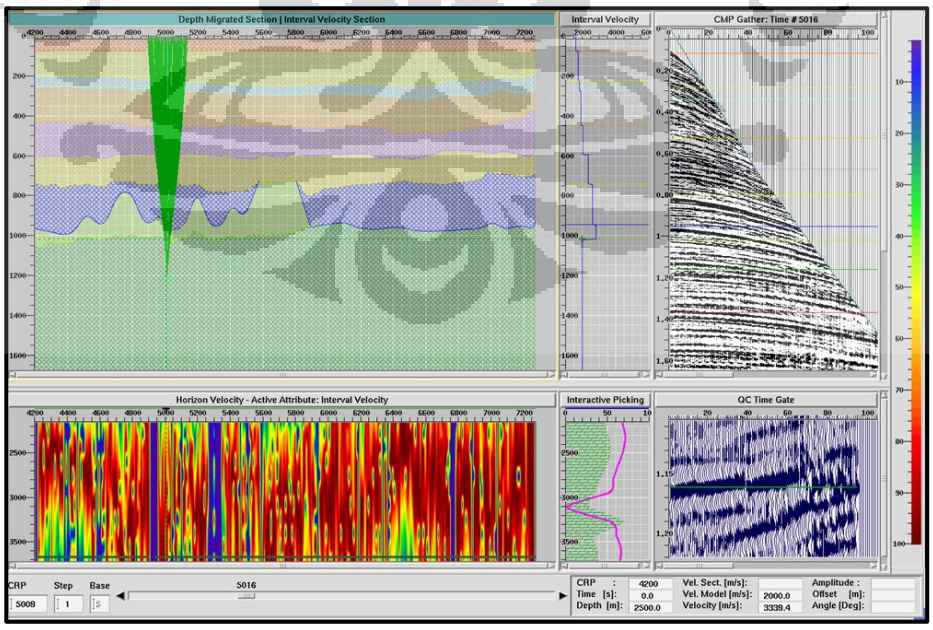

Figure 4.1 Coherency Inversion in Horizon-9

The initial model, both velocity and depth, is necessary to be determined properly. It is caused that the refinement step is using the previous model, initial model, as the references to calculate the new model. If the initial model is extremely inaccurate, it leads to get large error for the next step and always accumulated.

The velocity analysis of isotropic PSDM is focused on near-offset which using 30 degree mute. As shown in figure 4.2, the red line of that figure is the 30 degree mute which is boundary analysis of isotropy and anisotropy. The reflector event inside 30 degree mute requires to be flattened before continuing to the anisotropy stage. The flat reflector can be obtained by picking the appropriate isotropic interval velocity.

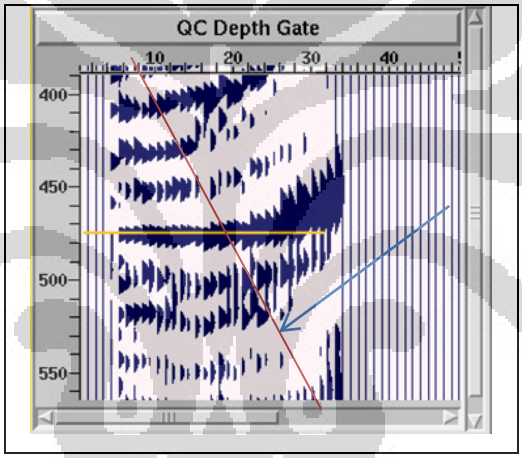

Figure 4.2 Muting the depth gather on 30 degree

The isotropic velocity model for 30 degree mute is closely predicted to the accurate velocity model. The event at near-offset of the depth gather is mostly flat, but in some area still showing non-flat event. In order to refine the velocity and depth model, the RMO analysis and horizon-based tomography are performed.

Figure 4.3 portrays the initial velocity model and final isotropic velocity model. As can be seen, the final model is not too much different with the initial model. It seems that the final velocity model is more subtle rather than the initial model and as if the refinement process is only smoothing the initial model. It is

caused the refinement process based on initial model in analyzing velocity-depth model. Hence, the initial model completely influences the next stage.

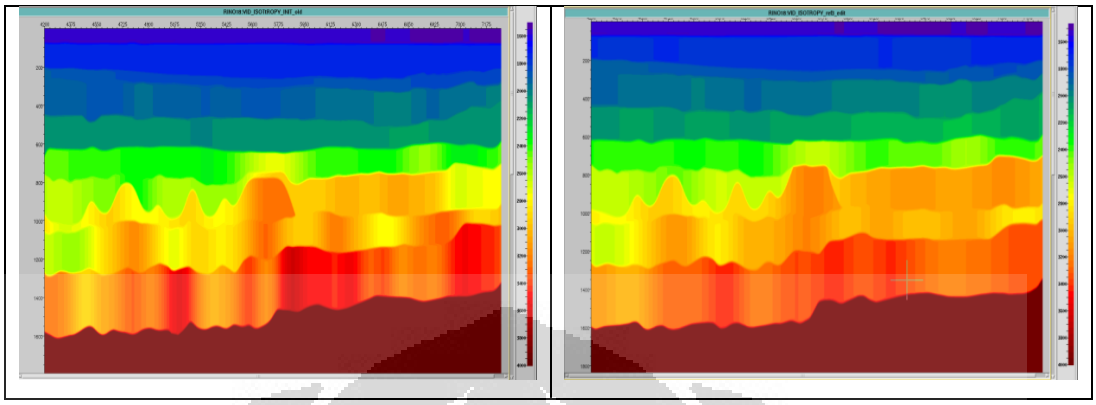

Figure 4.3 Initial isotropic interval velocity model and final isotropic interval velocity model

The refinement step is performed simultaneously as many as 3 iterative. The interval velocity model is already optimum when the differences of the model before and after refinement step is relatively small. Figure 4.4 shows the comparison between gather of refinement-1 and refinement-3. Both pictures are almost similar, but if observed in detail, there is a difference on those figures.

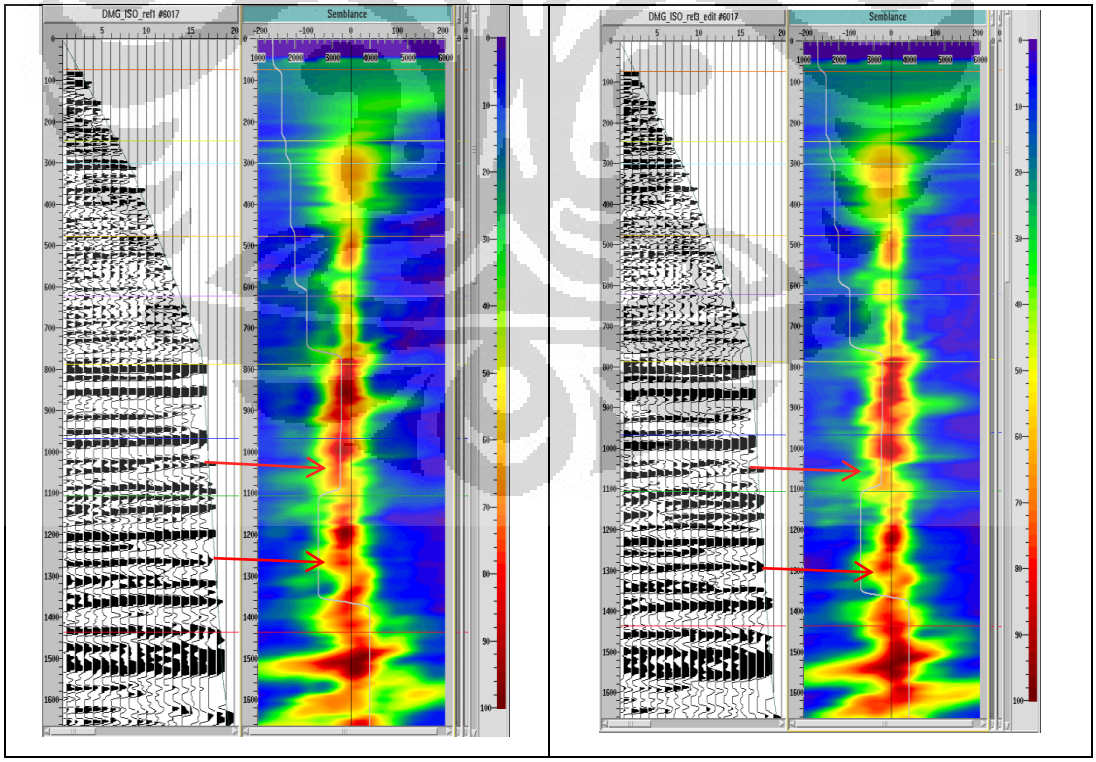

Figure 4. 4 Depth Gather CRP-6017, refinement-1 (left) and refinement-3 (right)

The position of semblance on figure 4.4 is different whereas the flat gather indicates the maximum semblance is focused on the center of zero moveout line, the vertical black line on semblance. The figure on the right side shows the maximum semblance more focus rather than the figure on the left side. The accurate velocity model on migration completely drives the result of depth gather. Once the depth gather is in flat condition, the result of stack section gives better reflection.

Due to the velocity analysis is performed in less than 30 degree mute, the reflector at the far-offset is not flat, hockey stick effect. Despite the hockey stick still exist, the gather needs to be stacked from near-offset until far-offset in order to involve all information of seismic record. Figure 4.5 shows a certain part of seismic stack section which stacked from near-offset until far-offset.

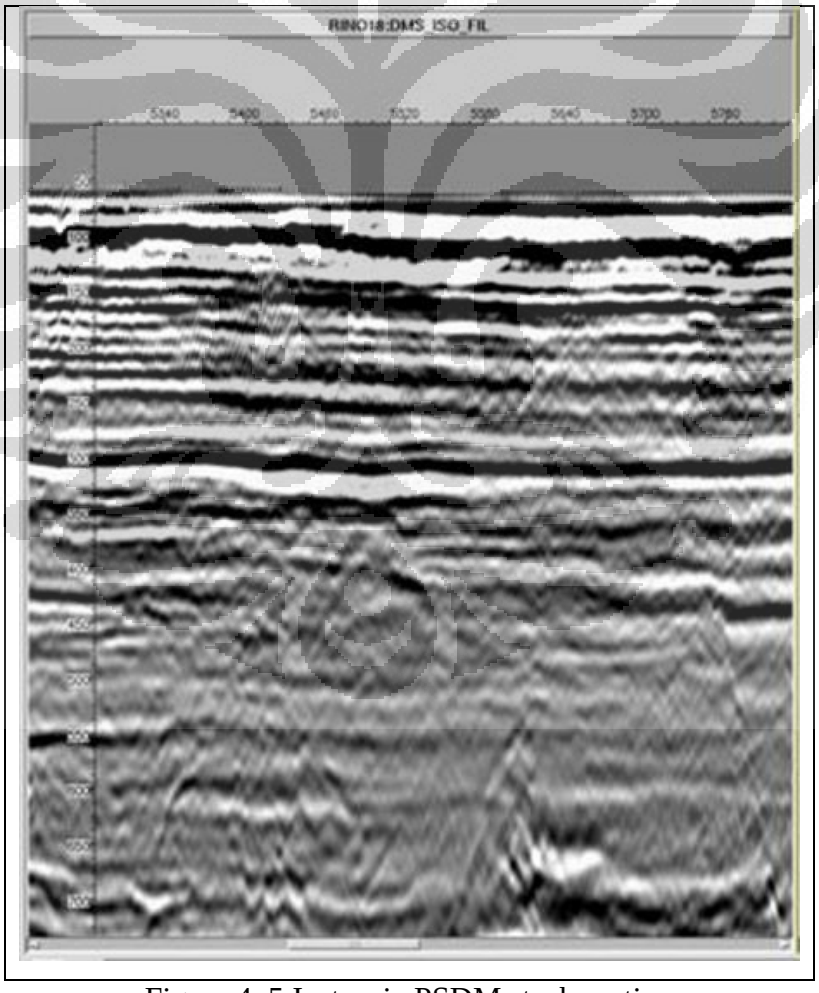

Figure 4. 5 Isotropic PSDM stack section

4.2 Comparing Isotropic PSDM with Anisotropic PSDM

Despite the isotropic PSDM successfully yields the flat gathers at near-offset, another challenge comes up. There are 2 obstacles that need to be solved in isotropic PSDM section which are miss tie between seismic horizons against well markers and the non-flat reflector event in the depth gather at the far-offset. The miss tie between seismic horizons against well markers is caused by different velocity between seismic velocity and sonic velocity. In addition, the gather after isotropic PSDM is already flat at the near offset, but it is not flat at the far-offset which still remains non-flat reflector event. The non-flat reflector is due to the anisotropy effect, or referred as hockey stick effect.

In order to deal with those cases, Thomsen's parameters, which are δ and ε, play their role. δ parameter corrects the P-wave velocity in near-vertical direction and it has the direct correlation with anisotropic interval velocity. Meanwhile, ε parameter corrects the hockey stick effect at the far offset. So that the strong reflection can be obtained after the gathers stacked.

The final anisotropic velocity section where it passes 2-iterative process is depicted in figure 4.6. Initial anisotropic velocity model is generated by transforming δ parameter and isotropic velocity model. The final model is firstly defined before defining the final model of ε. δ parameter as one of variables that has influence in transforming isotropic interval velocity to anisotropic interval velocity. This velocity model is necessary to match the seismic horizon to well marker. In the process of matching seismic against well, the isotropic interval velocity of seismic is scaled down to anisotropic interval velocity in order to match to the well. Since the well is more represent the true condition rather than seismic.

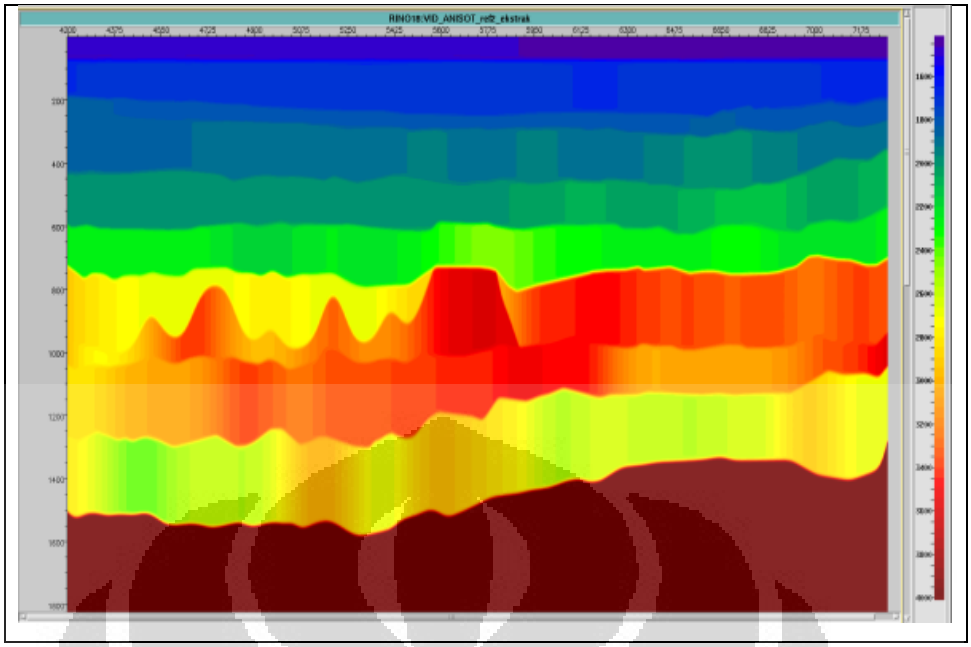

Figure 4. 6 Final anisotropic velocity section

The model of anisotropic velocity, δ, and ε are then used as input of anisotropic PSDM, besides time gather. The depth migrated gather is then analyzed whether the reflector at gather is flat or not. The semblance is used as the control of flatten gather as depicted in figure 4.7.

As can be obviously seen in the red circle of figure 4.7 a.), the hockey stick effect is still exist in depth migrated gather at the far-offset. The yellow circle of the semblance also indicates that the focus of the semblance is still away from zero moveout line. The position of the dominant semblance is located at the right side of zero moveout line whereas it indicates the gather is overcorrected.

Meanwhile, after anisotropic PSDM performed with the final model of velocity, δ, and ε, the hockey stick as well as the reflector depth level of depth migrated gather is corrected as depicted in figure 4.7 b). It means that anisotropic velocity, δ, and ε works to correct such a thing. As quality control, the semblance of figure 4.7 b) indicates that the dominant semblance is focused on zero moveout line which means the gather is already flat. It is the final anisotropic depth migrated gather.

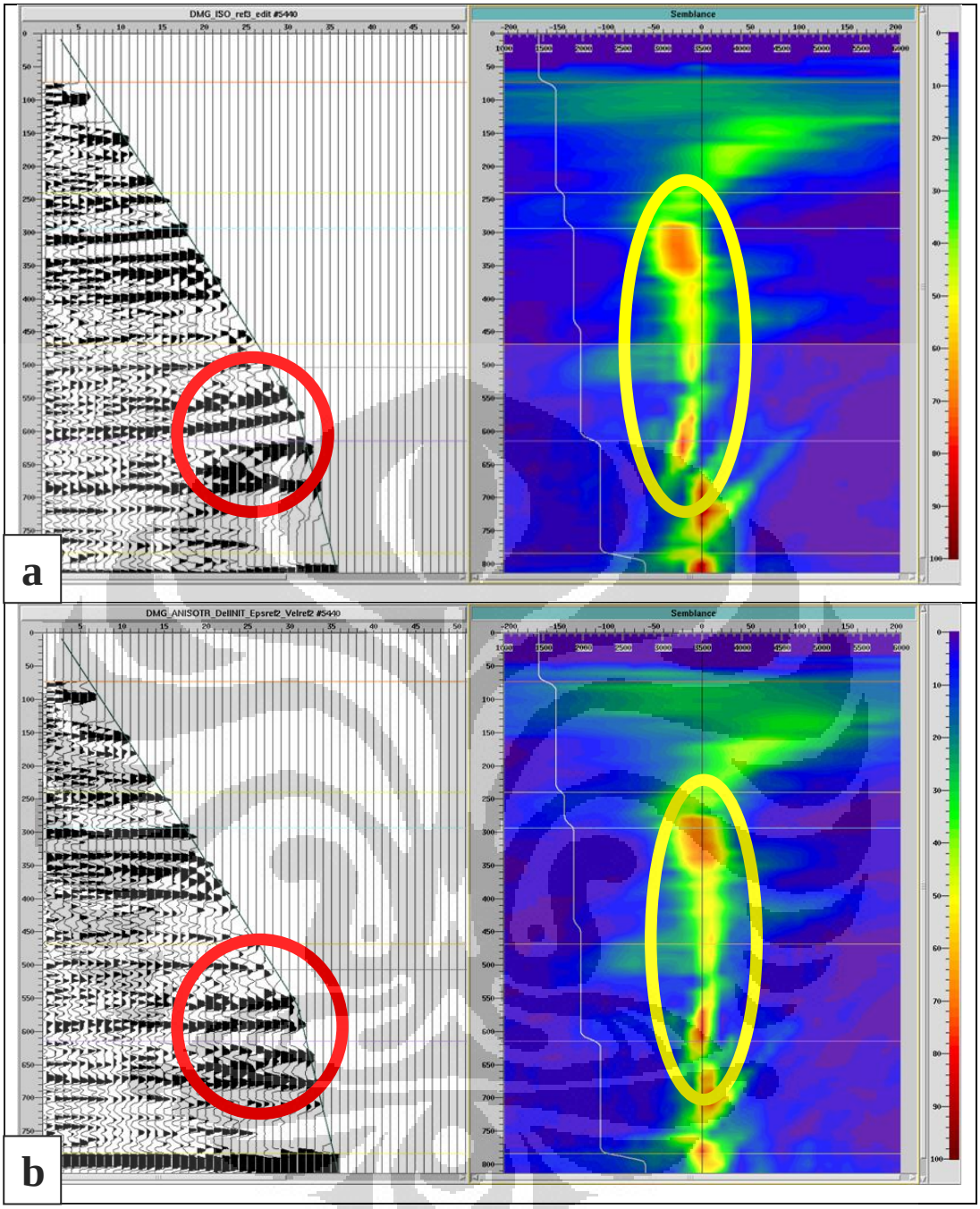

Figure 4. 7 CRP-5440 of depth migrated gather and QC semblance as result of a) isotropic PSDM and b) final anisotropic PSDM

The isotropic and final anisotropic depth migrated gather are then stacked at the far-offset with the same mute function. Figure 4.8 and figure 4.9 are the isotropic depth migrated stack section and the anisotropic depth migrated stack section, respectively. Those figures are taken at well and surrounding area.

Figure 4.8 shows that the seismic horizon as the result of interpretation in depth migrated section is not tie with the well marker, as can be seen in the red circle and the blue narrow. The green short lines are the well markers and the seismic horizons are showed by yellow, blue, green, and red long line. The red circle indicates the large miss of seismic horizon against well marker while the blue narrow indicates the small miss-tie.

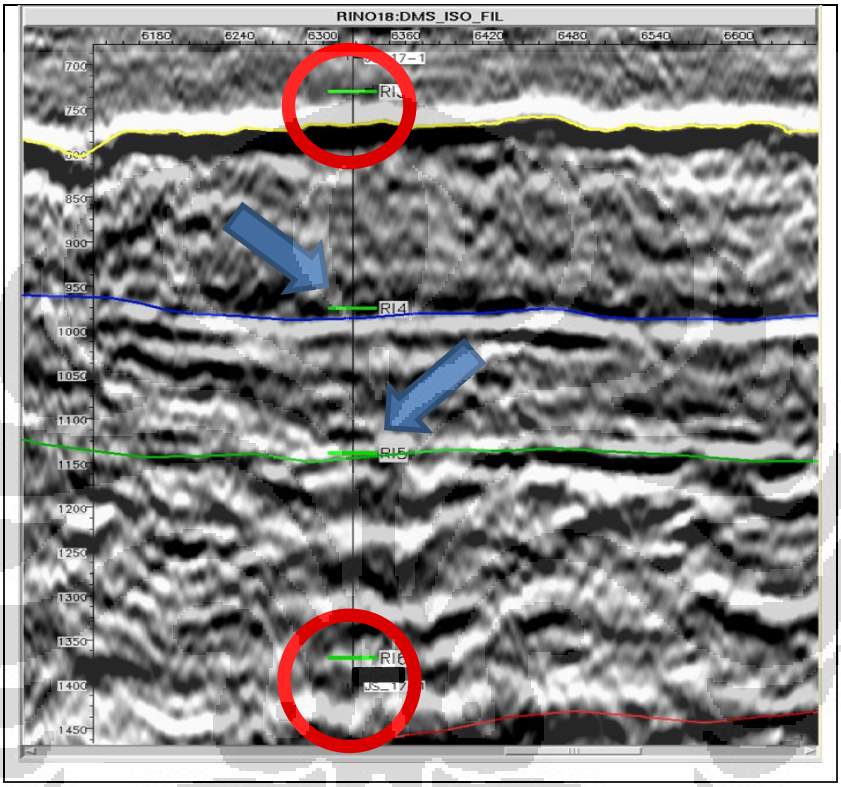

Figure 4.8 Miss-ties between seismic section and well marker in isotropic PSDM

As consequence of anisotropic interval velocity and δ in the process of migration, the seismic horizon is match to the well marker. Figure 4.9 depicts the seismic horizon which already matches with the well marker as indicated by the blue circle.

In the other side, the anisotropic PSDM also offers the advantageous which are the strong and continuous amplitude reflection in seismic section. It can be reached once the hockey stick effect is corrected. Figure 4.10 shows the comparison between the section of isotropic and anisotropic PSDM in another specific part. It can be clearly seen that the anisotropic PSDM section has the number of superiorities compared to isotropic PSDM section. There are 3 main

different things in the result of anisotropic PSDM from isotropic PSDM which are the strong reflector, the pattern of fault, and remove the random noise.

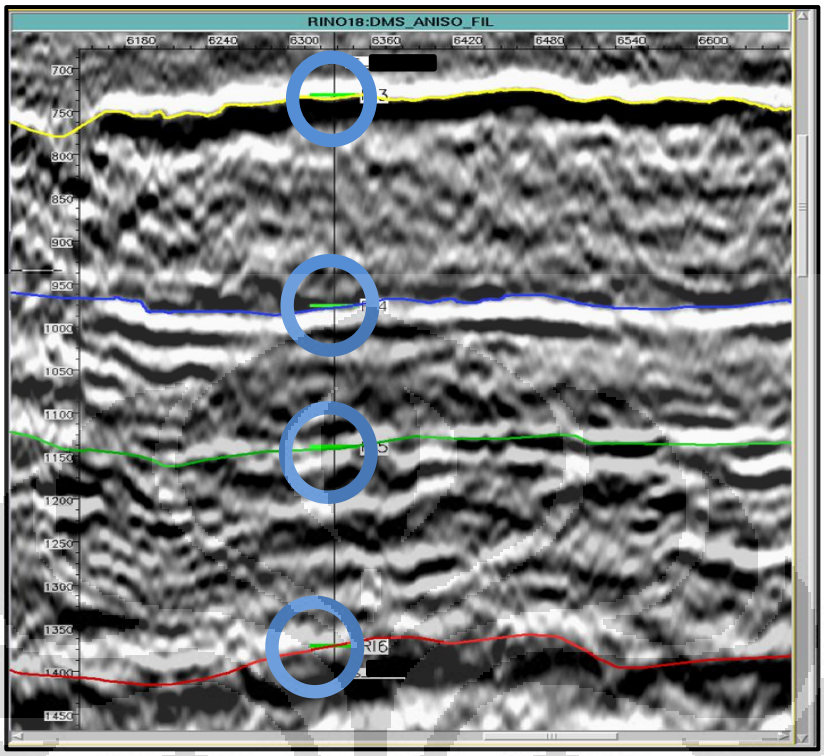

Figure 4.9 Anisotropic PSDM ties the seismic-to-well data

The blue narrow number 1 shows the strong reflection on the figure 4.10 b) compared to the figure 4.10 a) which the amplitude character on that area is adequate low. In addition, the surrounding area of that strong reflection indicates the removed random noise. Figure 4.10 a) shows the presence random noise on the stacked section. In contrast, figure 4.10 b) the noise is relatively pushed.

The other advantageous is in figure 4.10 a), it exhibits unclear faults on the stack section which indicated by blue narrow number 2 and 3. Fortunately, the pattern of those faults is solved by anisotropic PSDM. The continuous of faults clearly appears on the anisotropic PSDM section. On the blue narrow number 2 of figure 4.10 b), it shows the reflector on the surrounding area of the fault is somewhat revealed that also makes the continuity of the fault clearly seen.

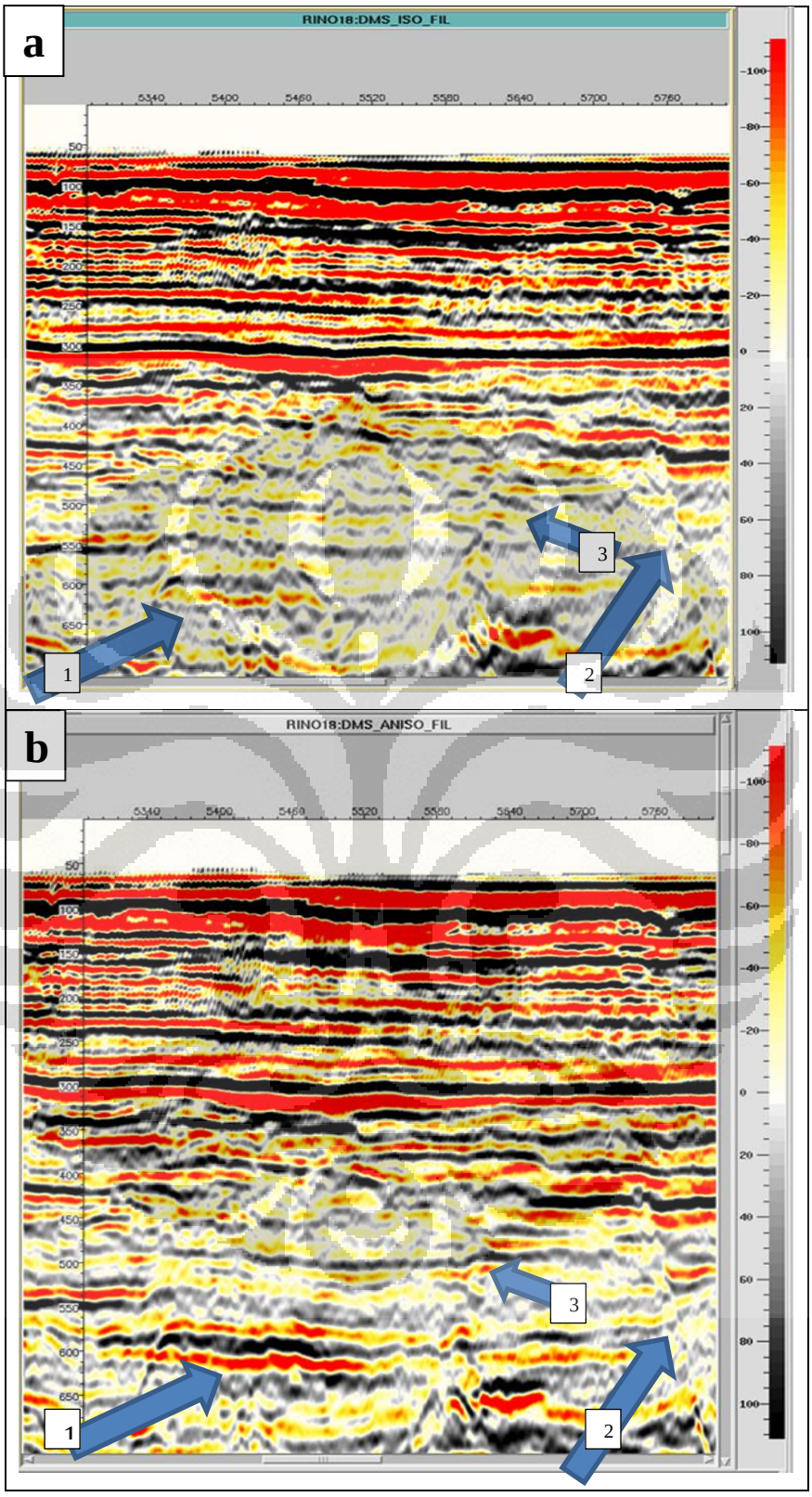

Figure 4.10 Stack section comparison between a.) Isotropic PSDM and b.) Anisotropic PSDM

Meanwhile, the fault that exhibited by blue narrow number 3 indicates the different pattern of fault. The fault on isotropic PSDM section is completely blurred and nothing can be seen on it. Conversely, the anisotropic PSDM section shows the fault that more clear compared to isotropic PSDM section. It can be seen that the fault on anisotropic PSDM section shows the firm pattern and diverges 2 faults on the upper part.

The better image quality of anisotropic PSDM section compared to isotropic PSDM section can be reached due to the appropriate interval epsilon used as input in migration. It is since when the reflector at the far-offset is flattened and then stacked, it yields stronger reflection image rather than the reflector that still remains non-flat reflection at the depth gather once it is stacked. The existence of hockey stick effect is flattened by ε parameter. As depicted in Figure 4.7, the isotropic depth migrated gather shows the hockey stick is exist at the far offset and in the anisotropic depth migrated gather is already corrected when the δ and ε already set on.

CHAPTER 5
CONCLUSIONS AND RECOMMENDATIONS

5.1 Conclusions

There are some conclusions that had been reached after doing the research of anisotropic prestack depth migration, those are:

1. As the best solution in imaging complex geological structure that has strong lateral variation, anisotropic PSDM yields significant improvement in the quality of seismic image and positioning rather than isotropic PSDM.
2. Prestack depth migration involving Thomsen's parameters in velocity model, anisotropy assumption, have proved to be a worthwhile process to tie the seismic data against well data. In this study, ε interval range is from 0 to 0.17387 while δ interval range is from -0.07459 to 0.30541.
3. The differences image section between isotropic PSDM and anisotropic PSDM are the quality event reflector that includes strong reflection, the removed random noise as well as clear fault pattern, and its positioning whereas anisotropic PSDM shows better image section.

5.2 Recommendations

As known, velocity model plays the main role in migration process. The existence of noise in the gather yields ambiguity, or even result inaccurate, in building the interval velocity. Therefore, time gather as the input of PSDM extremely needs to pass the preconditioning step in order to push the noise as minimum as possible. In addition, in order to clearly look the anisotropy effect on seismic data, seismic survey should consider very long offset survey whereas the ratio of depth versus offset is 1:1.5.

REFERENCES

Alkhalifah, T., Tsvankin, I., Larner, K., Toldi, J. (1996). Velocity Analysis and Imaging in Transversely Isotropic Media : Methodology and A Case Study. The Leading Edge 15, No. 5, 371 – 378.

Alkhalifah, T., Tsvankin, Ilya. (1995). Velocity Analysis for Transversely Isotropic Media: Geophysics 60, 1550 – 1556.

Bastian. (2010). Prestack Depth Migration Anisotropi *pada* Data *Seismik* 2-D. *Tugas Akhir*: Institut Teknologi Bandung

Chun, J.H. and Jacewitz, C. (1981). Fundamentals of Frequency-domain migration: Geophysics 46, 717-732.

Claerbout, J. F. (1985). Imaging the Earth's Interior, *Blackwell Scientific Publications*.

Fagin, S., (2002). Model-Based Depth Imaging, *SEG Course Notes Series* 10, Tulsa.

Grechka, Vladimir, Tsvankin, Ilya. (1998). Feasibility of Nonhyperbolic Moveout Inversion in Transversely Isotropic Media, Center for Wave Phenomena Colorado School of Mines

Kjartansson, E. and Rocca, F. (1979). The Exploding Reflector Model and laterally Variable Media: *Stanford Exploration Project Report* 16, Stanford University.

Kosloff, D., Sherwood, J., Koren, Z., Machet, E., Falkovitz, Y. (1996). Velocity and Interface Depth Determination by Tomography of Depth Migrated Gathers. Geophysics 61, 1511-1523.

Landa, E., Thore, P., Koren, Z. (1991). Interpretation of Velocity Estimates from Coherency Inversion : Geophysics 56, 1377 – 1383.

Lawton, D. (2001). Slip-Slidin' Away – Some Practical Implications of Seismic Velocity Anisotropy on Depth Imaging: The Leading Edge, 70 – 73.

Levin, F.K. (1971). Apparent Velocity from Dipping Interface Reflections: Geophysics 36, 510-516.

Loewenthal, D., Lu, L., Roberson, R., and Sherwood, J.W.C. (1976). The Wave Equation Applied to Migration: Geophys. Prosp., 24, 380-399.

Mavko, G., Mukerji, T., and Dvorkin, J. (1998). The Rock Physics Handbook. Cambridge University Press, Cambridge.

Officer, C. B. (1958). Introduction to the Theory of Sound Transmission with Application to the Ocean. McGraw-Hill Book Co.

Sheriff, R. E. (1991). Encyclopedic Dictionary of Exploration Geophysics: Soc. Expl. Geophys.

Sherriff, R.E. and L. P. Geldart. (1982). Exploration Seismology, Second edition, Cambridge University Press.

Sherwood, J. W. C., Chen, K. C., and Wood, M. (1986). Depths and Interval Velocities from Seismic Reflection Data for Low-Relief Structures: *Proc. Offshore Tech. Conf.*, 103-110.

Thomsen, L. (1986). Weak Elastic Anisotropy: Geophysics 51, 1954 – 1966.

Thomsen, L. (2002). Understanding Seismic Anisotropy in Exploration and Exploitation, Society Exploration Geophysicists, Tulsa.

Tsvankin, Ilya and Thomsen, L. (1994). Nonhyperbolic Reflection Moveout in Anisotropic Media : Geophysics 59, 1290 – 1304.

Winterstein, D. F. (1990). Velocity Anisotropy Terminology for Geophysicists. *Geophysics* 55, 1070-1088.

Yilmaz, O. (2001). Seismic Data Analysis Volume 1 & 2, Society of Exploration Geophysicist.

APPENDIX

Appendix A

Coherency Inversion

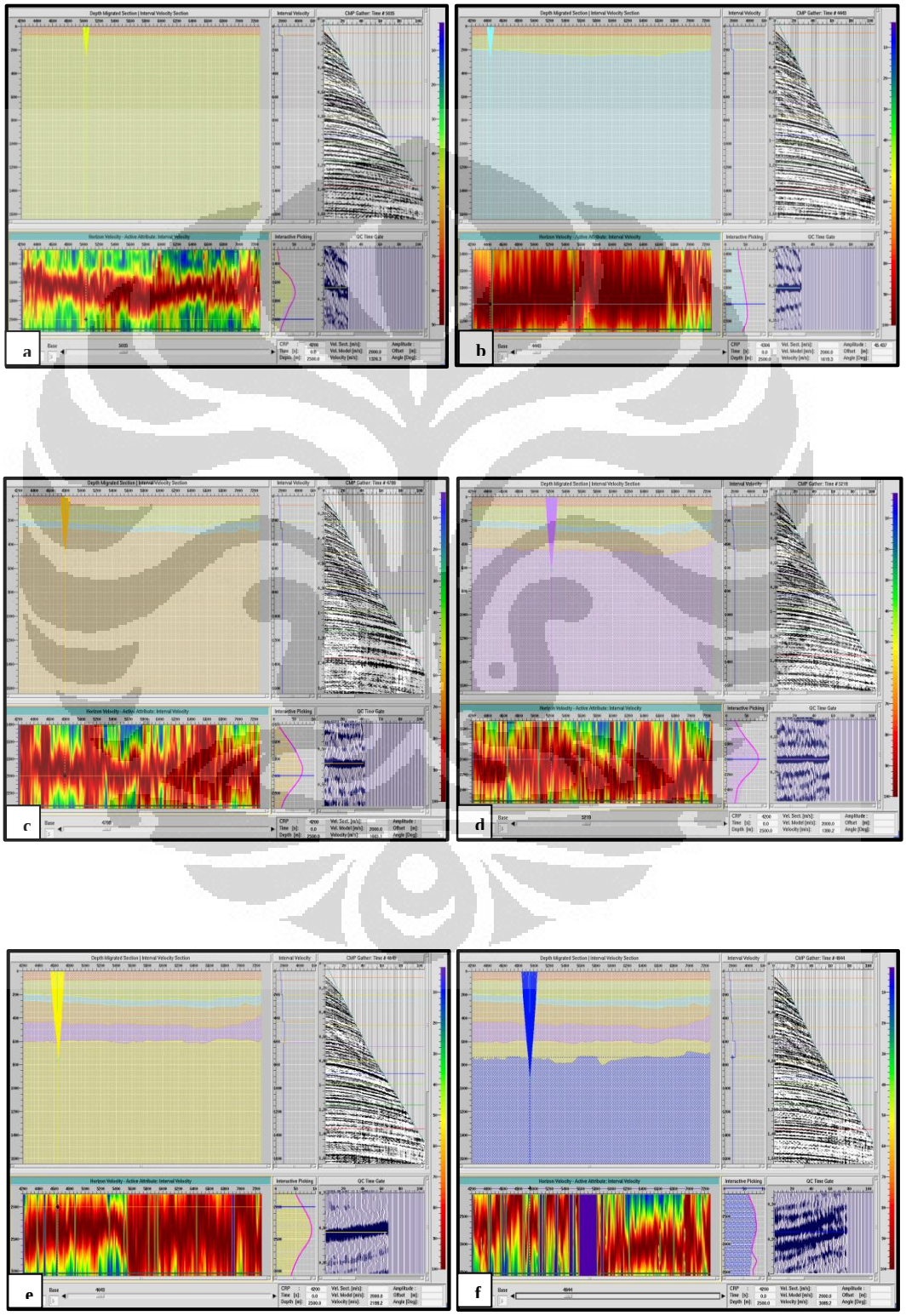

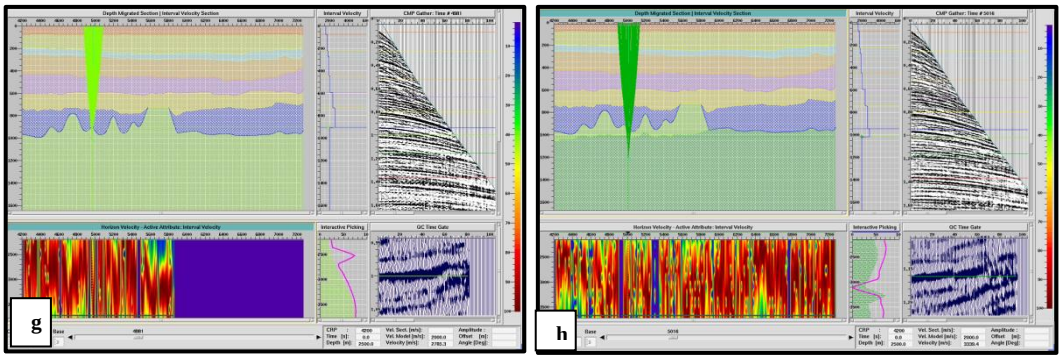

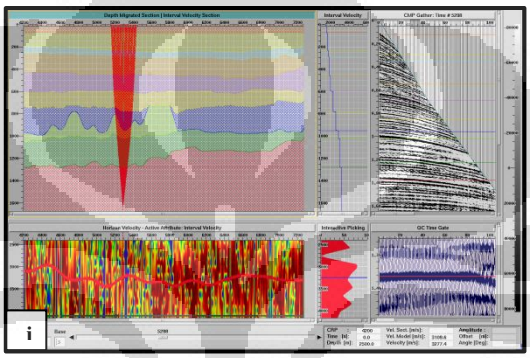

Appendix A Coherency inversion process at a) Horizon-2, b) Horizon-3, c) Horizon-4, d) Horizon-5, e) Horizon-6, f) Horizon-7, g) Horizon-8, h) Horizon-9, i) Horizon-10

Appendix B

Residual Moveout Analysis

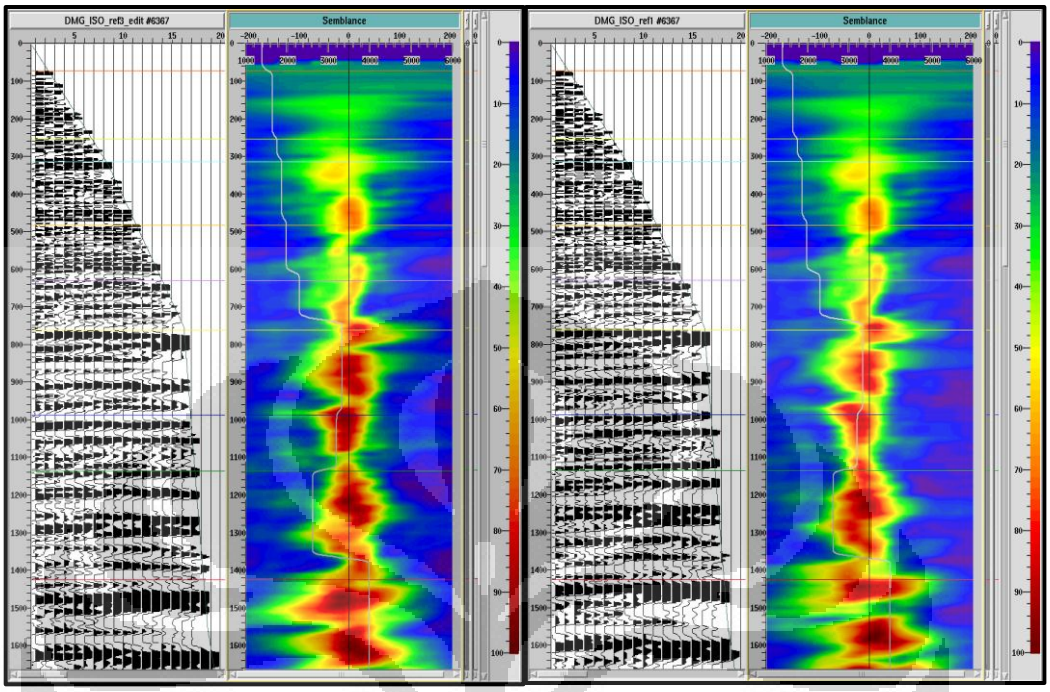

Appendix A-10 Depth Gather CRP-6367, refinement-1 (left) and refinement-3 (right)

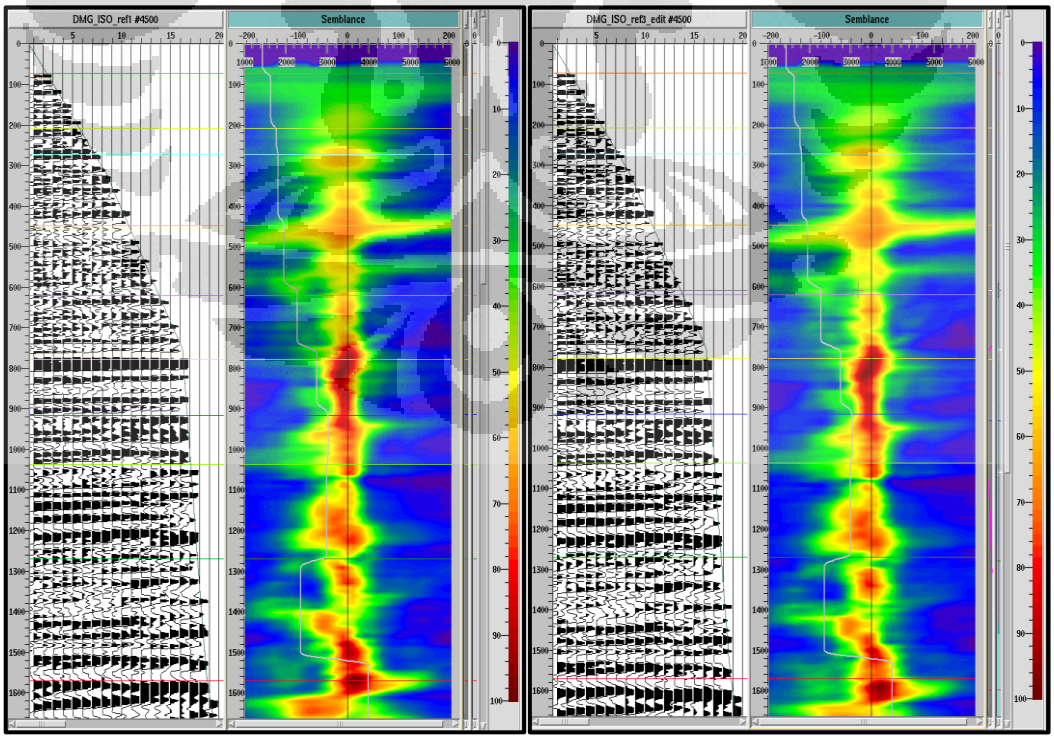

Appendix A-11 Depth Gather CRP-4500, refinement-1 (left) and refinement-3 (right)

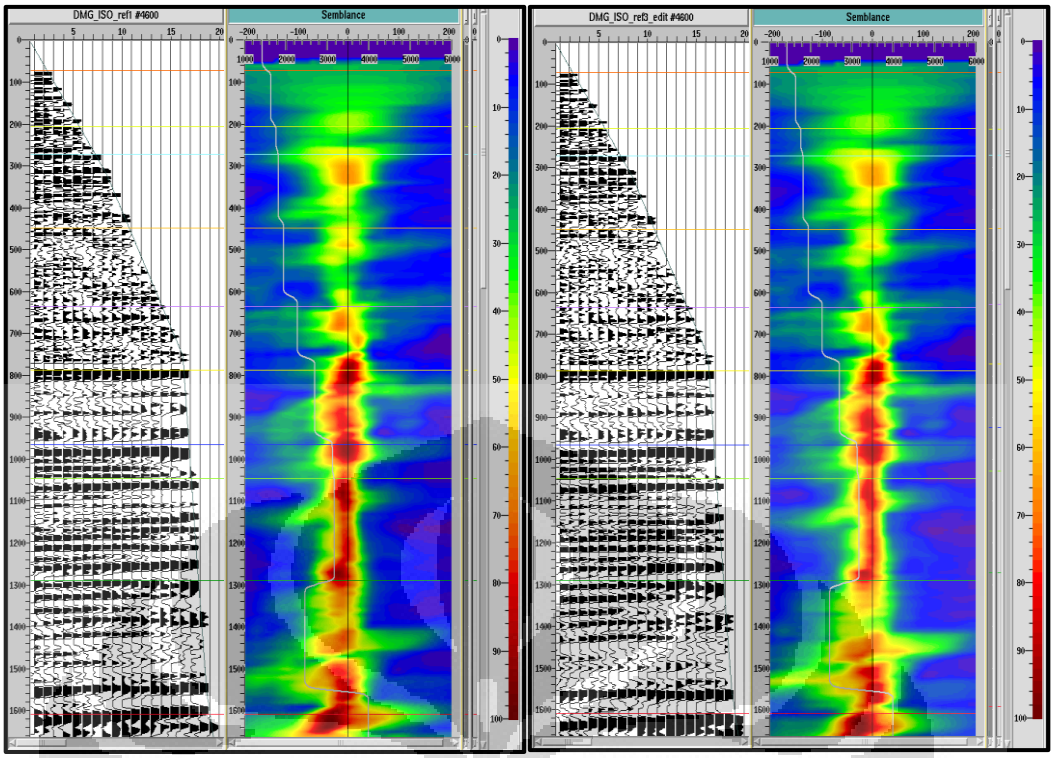

Appendix A-12 Depth Gather CRP-4600, refinement-1 (left) and refinement-3 (right)

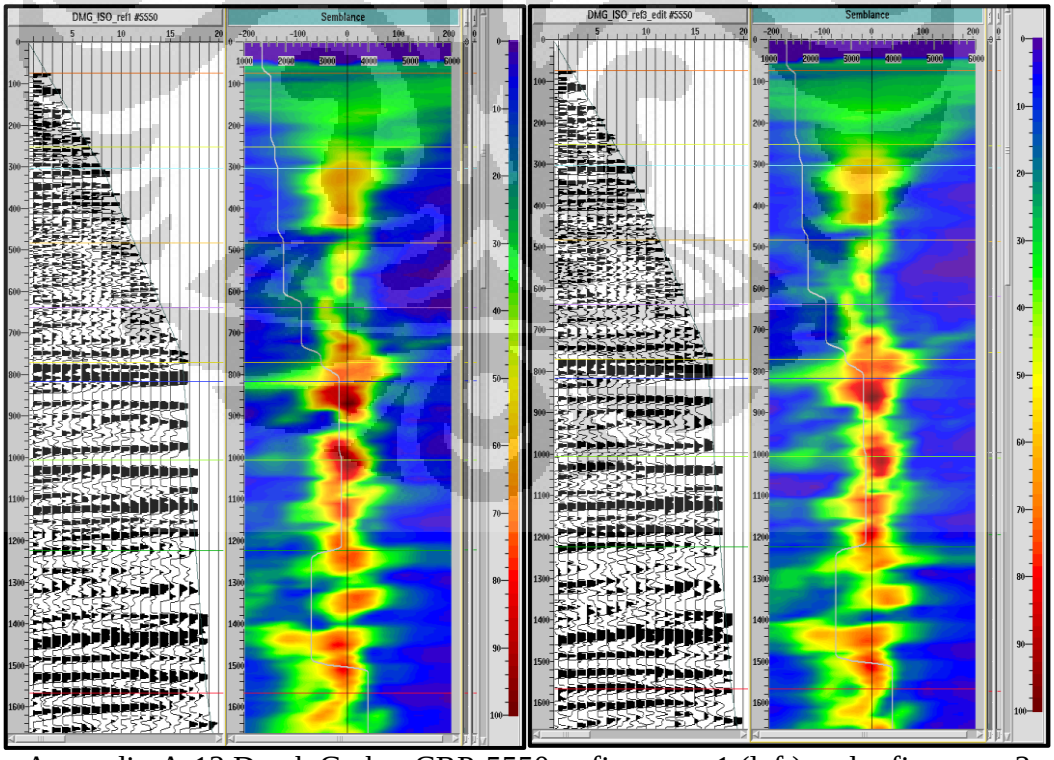

Appendix A-13 Depth Gather CRP-5550, refinement-1 (left) and refinement-3 (right)

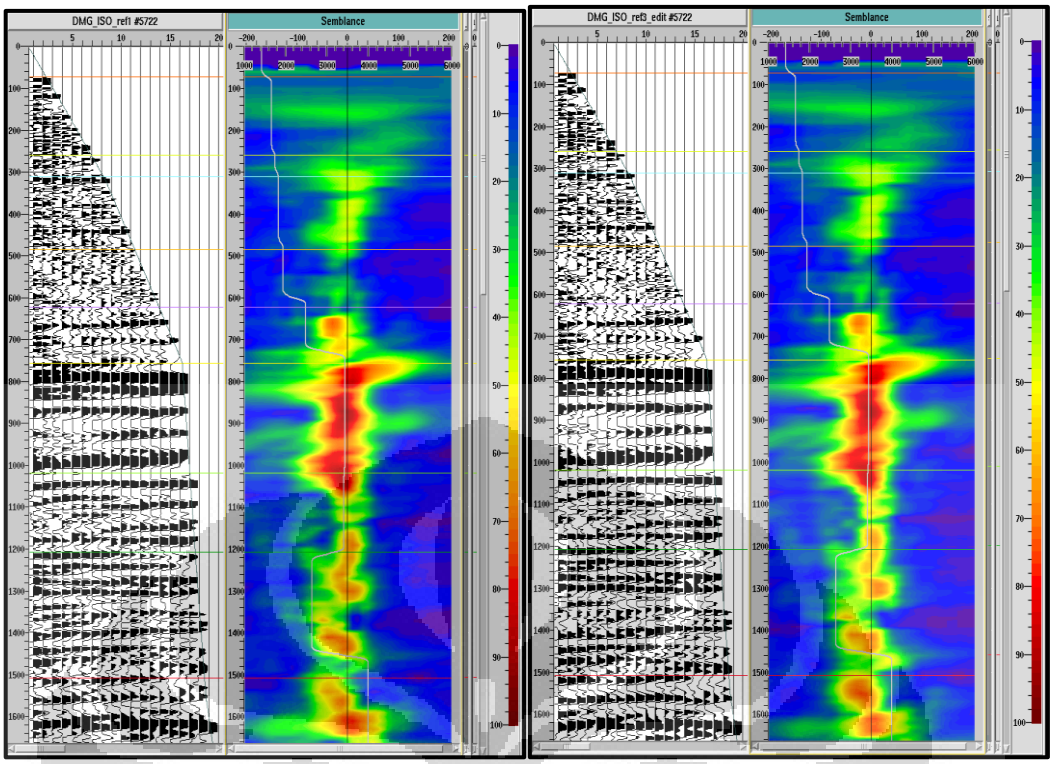

Appendix A-14 Depth Gather CRP-5722, refinement-1 (left) and refinement-3 (right)

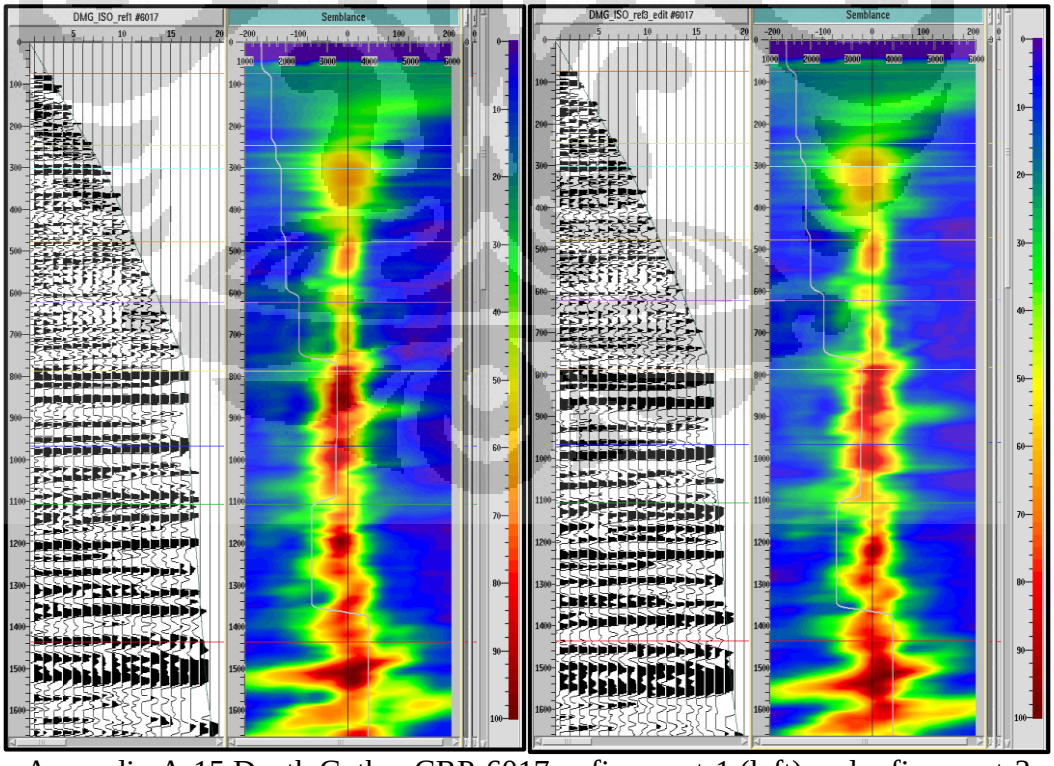

Appendix A-15 Depth Gather CRP-6017, refinement-1 (left) and refinement-3 (right)

Appendix C

Anisotropic Interval Velocity Refinement

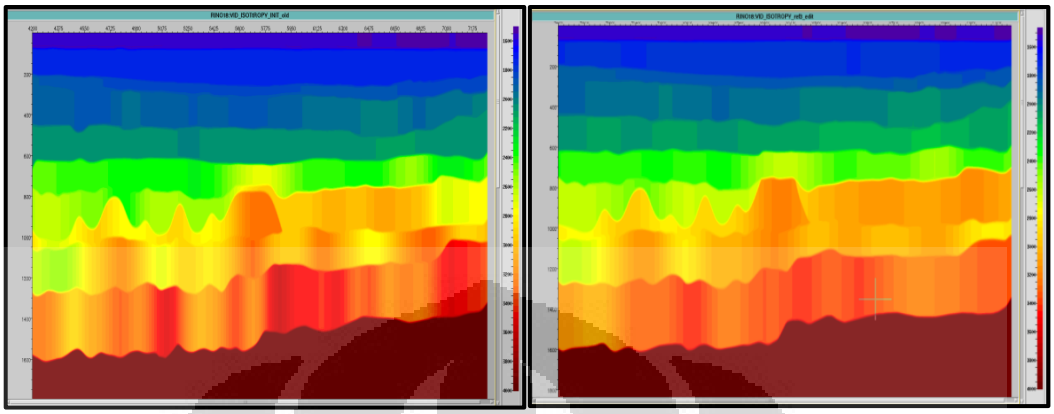

Appendix A-17 interval velocity model; initial isotropy (left) and final anisotropy (right)

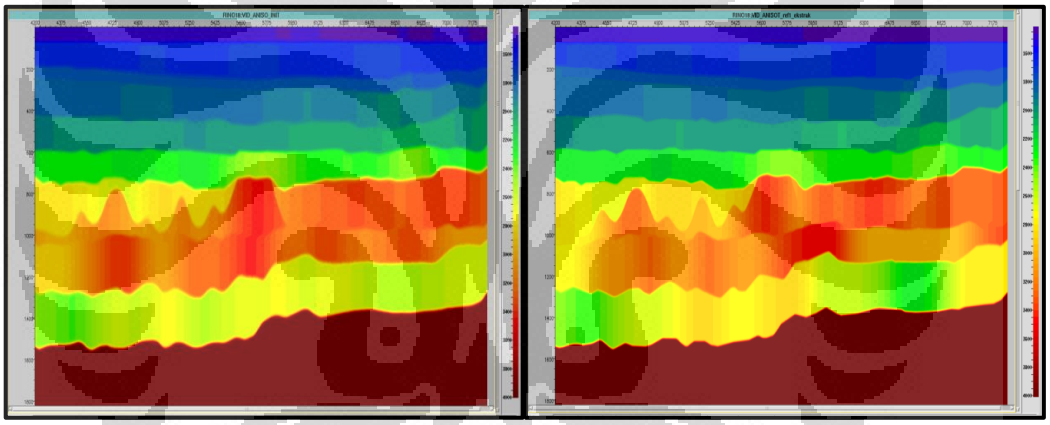

Appendix A-18 interval anisotropic velocity model; initial (left) and refinement-1 (right)

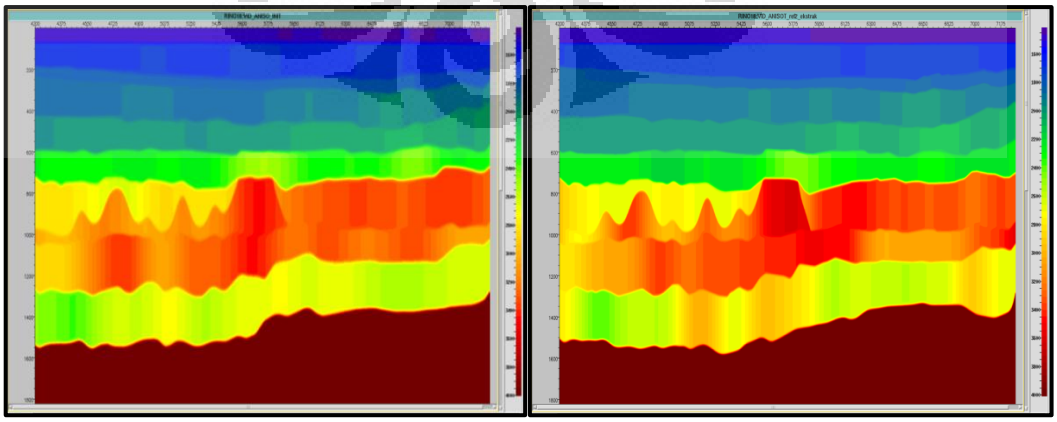

Appendix A-19 interval anisotropic velocity model; refinemet-1 (left) and refinement-2 (right)

Appendix D

Interval Epsilon

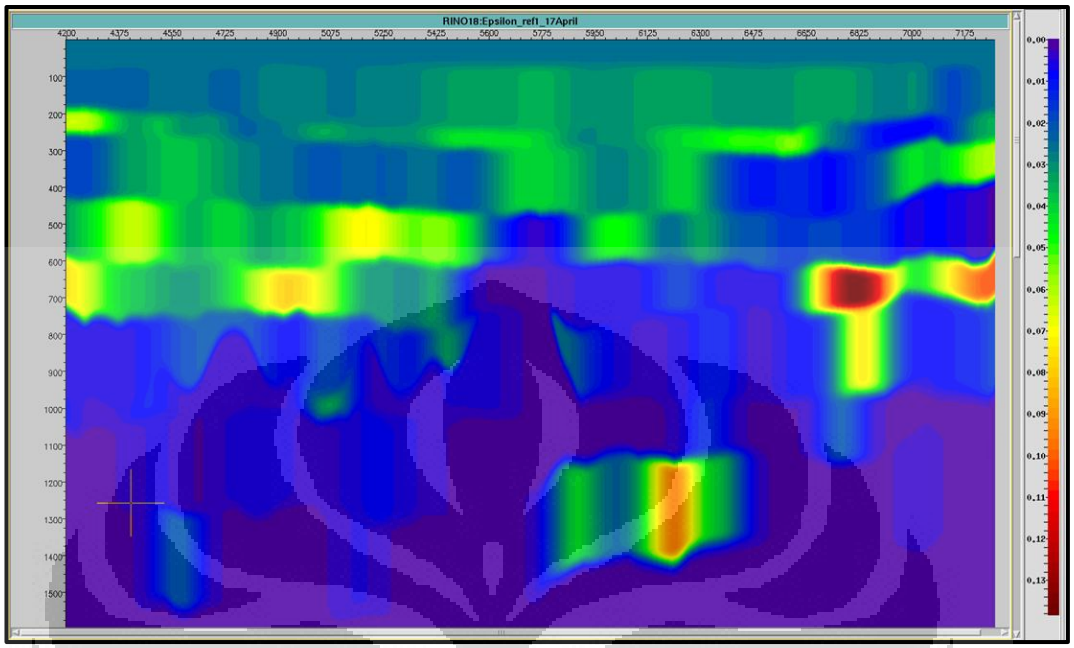

Appendix A-20 Interval epsilon section, refinement-1

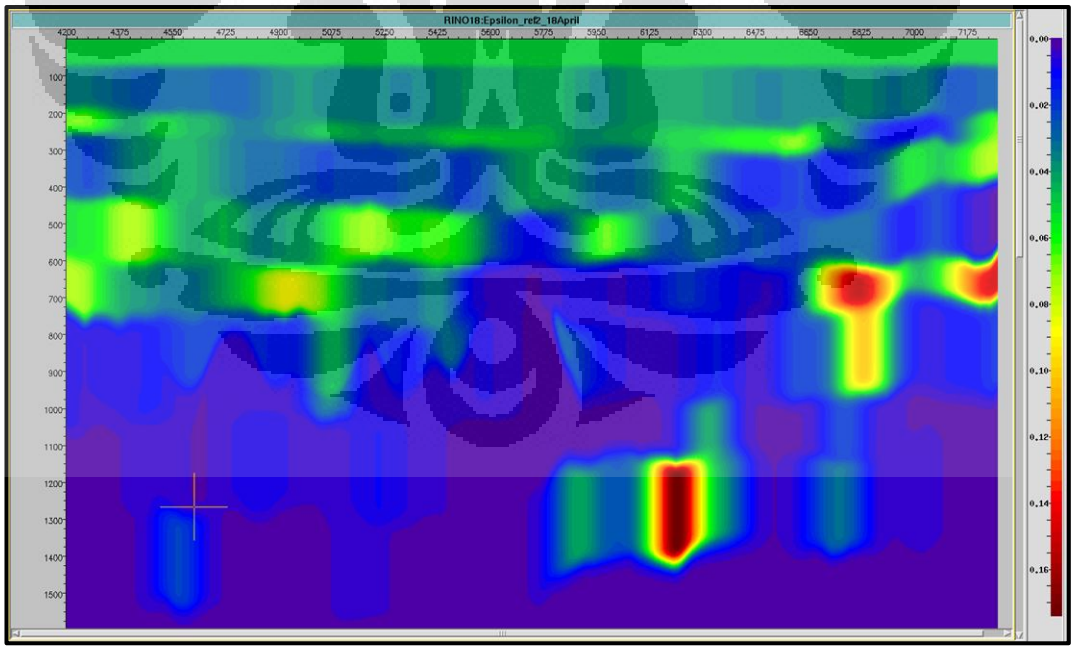

Appendix A-21 Interval epsilon section, refinement-2